Energy Strategy Reviews 61 (2025) 101818

Contents lists available at ScienceDirect

Energy Strategy Reviews

journal homepage: www.elsevier.com/locate/esr

Exploring European hydrogen demand variations under tactical uncertainty with seasonal hydrogen storage

Sebastian Emil Hummelen [a], Erlend Hordvei [a], Marianne Petersen [b,c], Stian Backe [a,d,*], Hongyu Zhang [a,e], Pedro Crespo del Granado [a]

[a] Department of Industrial Economics and Technology Management, Norwegian University of Science and Technology, Trondheim, Norway
[b] Department of Wind and Energy Systems, Technical University of Denmark, Lyngby, Denmark
[c] Siemens Gamesa Renewable Energy A/S, Brande, Denmark
[d] SINTEF Energy Research, Trondheim, Norway
[e] School of Mathematical Sciences, University of Southampton, Southampton, United Kingdom

ARTICLE INFO

M. Howells

Keywords:
Energy system modeling
Stochastic optimization
Tactical uncertainty
Seasonal storage
Hydrogen demand profile

ABSTRACT

Achieving a net-zero energy system in Europe by 2050 will likely require large-scale deployment of hydrogen and seasonal energy storage to manage variability in renewable supply and demand. This study addresses two key objectives: (1) to develop a modeling framework that integrates seasonal storage into a stochastic multi-horizon capacity expansion model, explicitly capturing tactical uncertainty across timescales; and (2) to assess the impact of seasonal hydrogen storage on long-term investment decisions in European power and hydrogen infrastructure under three hydrogen demand scenarios. To this end, the multi-horizon stochastic programming model EMPIRE is extended with tactical stages within each investment period, enabling operational decisions to be modeled as a multi-stage stochastic program. This approach captures short-term uncertainty while preserving long-term investment foresight. Results show that seasonal hydrogen storage considerably enhances system flexibility, displacing the need for up to 600 TWh/yr of dispatchable generation in Europe after 2040 and sizing down cross-border hydrogen transmission capacities by up to 12%. Storage investments increase by factors of 5–14, which increases the investments in variable renewables and improve utilization, particularly solar. Scenarios with seasonal storage also show up to 6% lower total system costs and more balanced infrastructure deployment across regions. These findings underline the importance of modeling temporal uncertainty and seasonal dynamics in long-term energy system planning.

1. Introduction

1.1. Problem context

Managing uncertainty is a key challenge in the energy transition. Methods like stochastic programming help address uncertainty across operational, tactical, and strategic levels [1]. This paper adopts uncertainty definitions on different time scales from logistical planning following Schmidt and Wilhelm [2].

- **Strategic**: Uncertainty affecting technology choice, location, and sizing of energy infrastructure to optimize long-term development for a sustainable and efficient energy system.
- **Tactical**: Uncertainty impacting production plans and energy storage inventory to optimize medium-term operations for seasonal supply–demand balance.
- **Operational**: Uncertainty influencing timely energy delivery to optimize short-term operations for meeting immediate needs and maintaining reliability.

Hydrogen is expected to play a key role in Europe's net-zero transition by 2050, especially where direct electrification is impractical [3]. It can also help balance variability from high shares of VRES [4]. Despite not being the most cost-effective or efficient storage option [5], this paper hypothesizes that hydrogen, particularly seasonal storage, can effectively manage tactical uncertainty and support long-duration energy balancing [6]. Hordvei et al. [7] explores investment planning for Europe's 2050 energy system, emphasizing VRES and electrolyzer expansion, but the study omits seasonal hydrogen storage and tactical uncertainty.

* Corresponding author at: Department of Industrial Economics and Technology Management, Norwegian University of Science and Technology, Trondheim, Norway.
E-mail address: stian.backe@ntnu.no (S. Backe).

https://doi.org/10.1016/j.esr.2025.101818
Received 13 January 2025; Received in revised form 25 June 2025; Accepted 31 July 2025
Available online 14 August 2025

Acronyms

BALMOREL	Baltic Model of Regional Electricity Liberalization
BESS	Battery energy storage systems
CCS	Carbon capture and storage
EMPIRE	European Model for Power System Investment with high shares of Renewable Energy
ENTSO-E	European Network of Transmission System Operators for Electricity
EU	European Union
H_2	Hydrogen gas
MILP	Mixed integer linear programming
PW	Power
PyPSA-Eur	Python for Power System Analysis - Europe
UK	United Kingdom
VRES	Variable renewable energy sources

1.2. Research gaps

Seasonal energy storage has been studied to explore the potential of hydrogen in Europe [8–12]. However, these studies either assume perfect foresight of future conditions or do not allow for energy storage between seasons. Moreover, current studies lack a thorough analysis of hydrogen demand profile assumptions, often based on uncertain projections [8,9].

The literature lacks studies modeling tactical uncertainty and analyzing seasonal hydrogen storage in capacity expansion models. Since real-world decisions must account for uncertainty, it remains unclear how seasonal storage investments influence VRES and related infrastructure.

1.3. Research objectives

This paper addresses two research questions:

1. How can seasonal energy storage be modeled in a stochastic multi-horizon capacity expansion model to account for tactical uncertainty?
2. What are the effects of seasonal energy storage on European investment planning for hydrogen and power infrastructure under different future scenarios when considering tactical uncertainty?

The main objectives of this paper are to (1) develop a multi-horizon capacity expansion model incorporating tactical uncertainty, and (2) apply it in a European case study to assess how seasonal hydrogen storage affects long-term investment decisions toward 2050. Tactical uncertainty includes variations in weather and energy demand, and the case study will compare results with and without the consideration of tactical uncertainty and seasonal storage.

A secondary objective is to examine how seasonal variations in hydrogen demand influence long-term investments. Demand profiles, driven by sector adoption in transport and industry [13], are uncertain. Thus, three scenarios are explored: winter peak (mirroring natural gas use [14]), summer peak, and constant demand. While future patterns may differ, the focus is on how these profiles affect the value of seasonal hydrogen storage under tactical uncertainty.

This paper extends EMPIRE [7] with seasonal hydrogen storage in a stochastic multi-horizon framework, enabling inter-seasonal planning under short-term and tactical uncertainties such as VRES availability and energy demand. The novelty lies in modeling seasonal uncertainty and assessing how different hydrogen demand profiles affect the European energy system. Practical implications include supporting investors and policymakers in identifying affected technologies and making robust investment decisions. The European case study also highlights the most suitable countries for seasonal hydrogen storage deployment.

1.4. Paper structure

The paper is structured as follows: Section 2 reviews research to further elaborate on gaps and contributions. Section 3 details our model extension and mathematical formulation in response to the first research question. Section 4 describes the case studies and data, while Section 5 presents and discusses the results in response to the second research question. Finally, the paper concludes in Section 6.

2. Literature review

This section presents current research in energy storage and hydrogen in capacity expansion models before presenting the research gaps and our contribution to the existing literature. There are many energy modeling tools to study future smart energy systems [15], and Table 1 provides a filtered overview of the models commonly used to address capacity expansion, hydrogen, storage, and uncertainty, serving as a foundation for the discussion that follows.

2.1. Uncertainty modeling in energy system planning

Building on the overview in Table 1, this study emphasizes the importance of uncertainty modeling in energy system planning. Accurately capturing both short- and long-term uncertainty is critical for robust investment and operational decisions [12]. Multi-horizon stochastic programming, applied in several recent studies [17–19], is the leading method for addressing multi-timescale uncertainty. Notably, Zhang et al. [20] introduced a model incorporating both temporal scales, while Zhang et al. [21] proposed efficient decomposition techniques.

Literature highlights the need for high temporal and spatial resolution, and scenario-based analysis, especially for modeling energy storage under variable renewables [22,23]. Capturing uncertainty in VRES availability and demand profiles is essential due to their strong interdependence with storage and production.

This study extends EMPIRE with seasonal storage and tactical uncertainty, enabling more realistic modeling of storage investments and operations under uncertain conditions.

2.2. Seasonal energy storage modeling

Building on the need to model uncertainty across timescales, this section reviews how seasonal storage is represented in capacity expansion models. Kaut [12] introduces a method for linking seasonal storage across representative periods in multi-horizon frameworks. However, this approach assumes perfect foresight, limiting its ability to capture tactical uncertainty.

A key challenge is the trade-off between modeling seasonal correlation and preserving uncertainty. Including full-year scenarios enables optimal storage use but removes uncertainty, while seasonally independent models like EMPIRE maintain stochasticity but restrict inter-seasonal energy flows, potentially underestimating long-term storage needs.

Abgottspon and Andersson [16] addresses this by using a stochastic tree to optimize hydropower operations under uncertain future prices, capturing tactical uncertainty without perfect foresight. While both studies focus on seasonal storage, one emphasizes investment planning and the other operational revenue, neither fully explores system-wide impacts or interactions with VRES investments.

Table 1
Model comparison for most relevant literature.

Article	Model	Stochastic	Linear	Seasonal storage	Hydrogen	Full year	Seasonal scale
Neumann et al. [8]	PyPSA-Eur-Sec		X	X	X	X	1
Strømholm and Rolfsen [11]	–			X	X		12.96
Abgottspon and Andersson [16]	–	X	X	X			1
Kaut [12]	HyOpt	X	X	X	X	Both	1, 6.48, 12.96
Hordvei et al. [7]	EMPIRE	X	X		X		
Kountouris et al. [9]	BALMOREL		X	X	X	X	1
Gabrielli et al. [10]	–		X	X	X	X	1
This paper	EMPIRE	X	X	X	X		2.17

Further highlighting the importance of hydrogen storage, Elberry et al. [24] show that geological hydrogen storage in Finland can reduce fossil fuel use and emissions while improving energy self-sufficiency. These findings support the need for integrated system-level models that combine hydrogen storage, uncertainty, and infrastructure planning.

2.3. Seasonal hydrogen storage in energy system models

To address this, Strømholm and Rolfsen [11] presents a multi-horizon MILP model for hydrogen production and storage using historical price data. It models one representative week per quarter to reduce complexity but focuses on single-facility revenue maximization, excluding system-wide investment impacts.

Fu and Hsieh [25] analyze Taiwan's energy system under various technology scenarios, comparing hydrogen storage with battery alternatives. They find hydrogen to be cost-effective in high-RES systems, reducing LCOE by 74%–78%. Sahraie et al. [26] use a stochastic MILP to minimize operational costs in a local energy system with dynamic hydrogen demand. Long-term hydrogen storage improves flexibility and buffers uncertainty from RES and load variability.

Several studies model seasonal hydrogen storage in full-year, multi-energy frameworks. Gabrielli et al. [10] explores storage profiles under varying capacities and VRES levels in a single-node model. Neumann et al. [8], Kountouris et al. [9], and Lux et al. [27] use PyPSA-Eur-Sec, BALMOREL, and Enertile, respectively, to assess hydrogen networks in Europe. While Neumann et al. [8] finds limited seasonal storage use, the others highlight the need for large-scale storage, estimating capacities up to 180 TWh in solar-heavy scenarios.

Hydrogen demand in Neumann et al. [8] is modeled from industry demand and zero-emission vehicle projections, assuming some energy demand in these sectors will be met by hydrogen. The demand has a daily profile repeated throughout the year, lacking seasonal variation. Kountouris et al. [9] does not specify a demand profile but similarly uses existing industry and transport data to project total demand for the coming decades.

Hydrogen demand in these studies is typically based on industry and transport projections, often assuming flat or repeated daily profiles without seasonal variation. Moreover, while these models offer high spatial and temporal resolution, they do not account for operational or tactical uncertainty in investment decisions.

This study complements existing work by explicitly modeling tactical uncertainty and exploring a wider range of seasonal hydrogen demand profiles, offering new insights into the role of hydrogen storage in long-term system planning.

2.4. Research gaps and contribution

The literature highlights a gap in modeling tactical uncertainty and analyzing seasonal hydrogen storage in capacity expansion planning. This study addresses both by quantifying how seasonal storage, under tactical uncertainty, influences investments in VRES and energy infrastructure. To do so, the EMPIRE model is extended to allow inter-seasonal energy transfer and incorporate varying hydrogen demand profiles and multi-timescale uncertainty.

This study makes two key contributions:

1. It enables inter-seasonal hydrogen storage in EMPIRE by linking representative seasons. The value of this feature is assessed by comparing scenarios with and without seasonal storage under varying hydrogen demand profiles.
2. It introduces tactical uncertainty through multi-stage subproblems in a multi-energy carrier model. Unlike existing hydropower-focused models, this approach incorporates hydrogen storage across multiple years in a European energy system context.

In summary, this study advances capacity expansion modeling by integrating seasonal hydrogen storage and tactical uncertainty. The extended EMPIRE model offers new insights into how hydrogen storage affects infrastructure investment and renewable integration under diverse demand conditions.

3. Methodology

This section presents the multi-horizon stochastic optimization model EMPIRE [18] with extensions to investigate the value of seasonal hydrogen storage, including endogenous consideration of tactical uncertainty.

3.1. Model overview

EMPIRE is a multi-carrier energy system model for planning operational and investment decisions in the European energy market. It represents the system as a network of nodes (markets with energy demand) and arcs (transmission links). The model minimizes total system costs by optimizing investments in production, storage, and transmission capacities, subject to constraints like capacity limits and VRES availability. Operational decisions follow from these investments and must meet hourly demand.

This study builds on the version of EMPIRE developed by Durakovic et al. [17], which includes explicit modeling of power and hydrogen carriers, their transmission networks, and demand. Power market modeling includes generation, storage, and cross-border flows (see [18]). The next section details the hydrogen market framework.

3.2. Hydrogen representation

Electrolysis is considered the only means of hydrogen production, meaning hydrogen production from natural gas reformers is excluded following the EU green hydrogen strategy [28]. Production must meet EU criteria for green hydrogen, including additionality and spatial and temporal correlation [29]. Although a 90% renewable grid exemption exists, it is not applied due to eligibility uncertainties. For details on the mathematical constraints for green hydrogen requirements, please refer to (A.6) and (A.7) in Appendix A [7].

As detailed in Durakovic et al. [17], hydrogen can be transported through pipelines, with net transfer capacity represented as arcs between nodes. Similar to the modeling of power transmission investments, this approach abstracts the physical size of the pipes, focusing solely on their net transmission capacity in tons per hour. Hydrogen can also be stored underground in salt caverns, aquifers, or depleted gas fields, with total potential energy storage capacity constrained by the country's geographical characteristics, as outlined in Section 4.2.

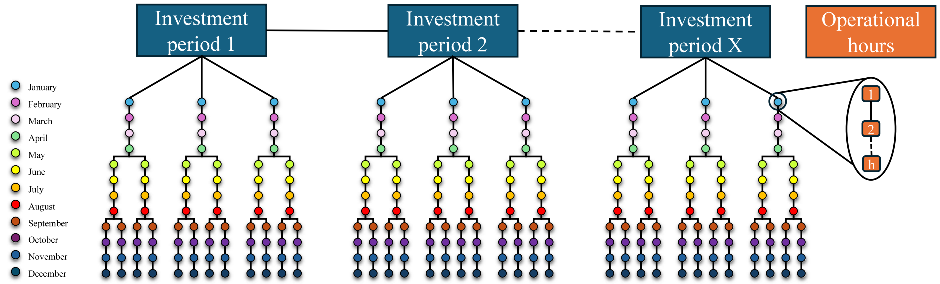

Fig. 1. EMPIRE model structure with short-term and tactical uncertainty. Each tree within an investment period represents a multi-stage stochastic problem.

3.3. Model decision structure

Fig. 1 illustrates that EMPIRE represents two time horizons: long-term strategic periods spanning multiple years and short-term operational periods with hourly resolution. The investment horizon concerns investment decisions for each long-term period, while the operational horizon involves operational decisions across several stochastic scenarios within each investment period. Investment decisions remain consistent across the operational scenarios embedded in the investment period, and these scenarios depict the hourly dispatch of assets for market clearing at each node.

3.4. Stochastic scenario generation

Stochastic scenarios are generated through random sampling of representative operational time windows with hourly resolution, as described in Backe et al. [30], to capture the uncertainty of stochastic parameters. These parameters include power and hydrogen demand profiles at each node for each operational hour and the production efficiency of VRES. Historical data realizations, scaled to represent a future investment period, are used. Data is sampled by selecting a starting hour within seasonal partitions, each covering a month or more across multiple years. For each investment period and seasonal partition, a unique starting hour is randomly chosen to construct the operational time window with hourly resolution, maintaining chronology and cross-correlation by using the same starting hour for all parameters in every investment period and seasonal partition. The duration of the operational time window is flexible, typically ranging from one day (24 h) to two weeks (336 h).

All scenarios are treated as equiprobable, meaning each is assumed to be equally likely. This is a standard approach when using historical data to represent future uncertainty in the absence of a known probability distribution. It ensures a balanced representation of possible outcomes without introducing bias.

To ensure the model accounts for high demand, peak operational windows are included by sampling random years and identifying two key hours: one with the highest demand at a single node, and one with the highest total demand across all nodes. For more details, see Backe et al. [30].

3.5. Model extensions

To address the inherent conflict between modeling seasonal energy storage and capturing tactical uncertainty, we introduce a novel extension to the EMPIRE model that represents a significant methodological advancement. Traditionally, short-term operational periods in capacity expansion models are treated as independent representative snapshots, limiting the ability to model intertemporal dynamics such as energy storage. In this work, we transform these operational periods into a coherent multi-stage stochastic decision framework, where representative periods are dynamically linked through energy storage levels.

Table 2 summarizes the extensions made to EMPIRE compared to Durakovic et al. [17]. This paper introduces a key innovation by incorporating the sequential nature of tactical uncertainty while preserving the long-term investment planning horizon, enabling a more realistic representation of seasonal storage across timescales. To manage complexity, hydrogen demand is treated as exogenous, and the model is solved using a rolling horizon approach (Section 3.8). Additionally, the model has been extended to incorporate the green hydrogen definition, as detailed in [7].

3.6. Multi-stage extension

In previous publications with EMPIRE [18,30,31], operational scenarios assume perfect foresight. Although each investment period includes several operational scenarios, the information about uncertain parameters is known with certainty within each operational scenario. Representative periods for energy demand and VRES availability are sampled by season, but no inter-seasonal storage transfer is allowed. This structure balances stochastic modeling with computational tractability.

Fig. 1 shows the extended model structure of EMPIRE used in this paper with tactical uncertainty. To incorporate seasonal storage, seasonal dependence is introduced by allowing energy storage levels to transfer from the end of one representative period to the beginning of the next through the coupling constraints shown in Section 3.7. Including seasonal storage introduces the challenge of perfect information over the entire operational period. This implies an unrealistic assumption that the model can optimize storage operations based on complete foresight of demand profiles and VRES production efficiency throughout each investment period. Tactical uncertainty is introduced by restructuring the operational decisions into a multi-stage decision problem. This incorporates tactical uncertainty between seasons by branching the stochastic tree at seasonal transitions.

However, since representative periods only capture a portion of their respective seasons, directly transferring the storage levels leads to underestimating the value of seasonal storage [12]. To address this, the net change in storage levels is scaled at the end of a representative period using a seasonal scale factor, assuming that the non-sampled hours within the season operate similarly to the represented hours. The scaling factor is determined by Eq. (1)

$$\delta = \frac{\text{Actual days per month}}{\text{Days per representative month}} = \frac{365/12}{14} = 2.17 \quad (1)$$

Relying solely on the net storage within a representative period to scale the transferred storage could introduce irregularities if the sampled period does not accurately reflect typical seasonal conditions [12]. To mitigate this issue, the number and length of representative periods is increased.

3.7. Mathematical formulation

The model structure of EMPIRE has been changed to a multi-horizon stochastic program with multi-stage operational decision problems. All regions in the model are represented by the set $\mathcal{N}$, and all investment periods are represented by the set $\mathcal{I}$. Each operational node ψ, circles

Table 2
Model extensions to EMPIRE in this paper compared to Durakovic et al. [17].

Model feature	Durakovic et al. [17]	This paper
Tactical uncertainty	No	Yes
Seasonal "Connection"	Storage fixed at 50% in first and last hour of a season	Storage is transferred from one season to the next
Hydrogen demand flexibility	Endogenous demand	Fixed demand per day
Long-Term horizon	Multi-horizon	Rolling horizon
Green hydrogen formulation	All electrolysis-based hydrogen	Adhering to EU green hydrogen definition [29]

in Fig. 1, is represented by $\mathcal{H}_\psi$ hours. $\mathcal{H}_\psi^{Start}$ and $\mathcal{H}_\psi^{End}$ represents the first and last hour of the operational node ψ. The first operational hour within an operational node is linked to the last hour in its parent node. The last operational hour in the final leaf nodes is linked back to the first operational hour in the initial operational node. This leads to a cyclic modeling of seasonal storage. The set of seasonal storage of energy carriers is defined as $\mathcal{B}^{c,seasonal}$, which is a subset of all storage units $\mathcal{B}^c$. In the following, the constraints related to seasonal storage are presented. For the complete formulation of objective function and constraints in the EMPIRE model, see Appendix A and Hordvei et al. [7].

$$y^{c,stor}_{b,n,h,i,\psi} = y^{c,stor}_{b,n,h-1,i,\psi} + y^{c,chrg}_{b,n,h,i,\psi} - y^{c,dischrg}_{b,n,h,i,\psi},$$
$$c \in \mathcal{C},\ b \in \mathcal{B}^c,\ n \in \mathcal{N},\ h \in \mathcal{H}_\psi \setminus \mathcal{H}_\psi^{Start},\ i \in \mathcal{I},\ \psi \in \Psi. \tag{2}$$

$$y^{c,stor}_{b,n,h,i,\psi} = y^{c,stor,0}_{b,n,h,i,\psi} + y^{c,chrg}_{b,n,h,i,\psi} - y^{c,dischrg}_{b,n,h,i,\psi},$$
$$c \in \mathcal{C},\ b \in \mathcal{B}^c,\ n \in \mathcal{N},\ h = \mathcal{H}_\psi^{Start},\ i \in \mathcal{I},\ \psi \in \Psi. \tag{3}$$

Eq. (2) ensures that, in an operational node ψ, the storage level $y^{c,stor}_{b,n,h,i,\psi}$ at the end of hour h equals to the storage level in the previous hour $y^{c,stor}_{b,n,h-1,i,\psi}$ plus the net charge in the current hour $y^{c,chrg}_{b,n,h,i,\psi} - y^{c,dischrg}_{b,n,h,i,\psi}$. Eq. (3) constraints the storage operation in the first hour in each node, where $y^{c,stor,0}_{b,n,h,i,\psi}$ is the initial storage level. These constraints apply to all storage units.

$$y^{c,stor,0}_{b,n,l,i,e} = y^{c,stor,0}_{b,n,h,i,f} + \delta(y^{c,stor}_{b,n,k,i,f} - y^{c,stor,0}_{b,n,h,i,f}),$$
$$c \in \mathcal{C},\ b \in \mathcal{B}^{c,seasonal},\ n \in \mathcal{N}, i \in \mathcal{I},\ e \in \Psi, f \in \Psi_e,$$
$$h \in \mathcal{H}_f^{Start}, k \in \mathcal{H}_f^{End}, l \in \mathcal{H}_e^{Start}. \tag{4}$$

Eq. (4) ensures that the initial energy storage level in the first operational hour in operational node ψ is passed from the last operational hour in its ancestor node. The Ψ_e is the set of the ancestor node to node e, and δ is the seasonal scaling factor of storage level from one operational node to the next. With the seasonal partition used in this paper, δ is defined in Eq. (1).

3.8. Rolling horizon investment perspective

To manage the complexity of long-term investment modeling with tactical uncertainty and seasonal storage, we use a rolling horizon approach [32]. This method divides the full problem into smaller, sequential subproblems, each covering a few investment periods. It enables detailed operational and investment modeling while keeping the problem computationally feasible. Complex features like multi-stage stochastic programming and inter-seasonal storage are included, with investment decisions passed between subproblems to ensure temporal consistency.

Fig. 2 illustrates this setup: the full horizon of X periods is divided into Z subproblems, each solving Y periods. The arrow illustrates that only investment decisions of the first period in the next subproblem are carried forward; investment decisions beyond the first investment period of the next subproblem inform the solution but are not retained. Operational decisions remain independent across periods. The process continues until all periods are covered, without a convergence criterion.

While this approach may lead to myopic decisions and underinvestment in long-term assets, it reflects real-world short-termism [33] and significantly reduces complexity [34]. To further simplify the model, spatial and technological detail is reduced (see Appendix H). A full assessment of these simplifications is left for future work.

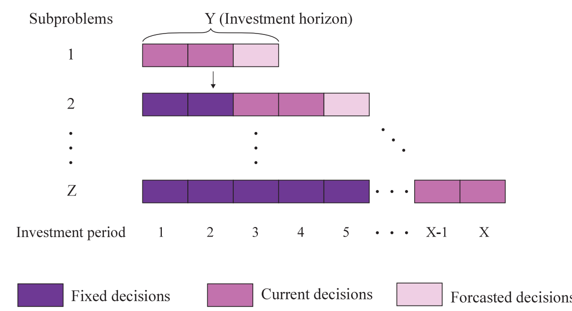

Fig. 2. Rolling investment horizon.

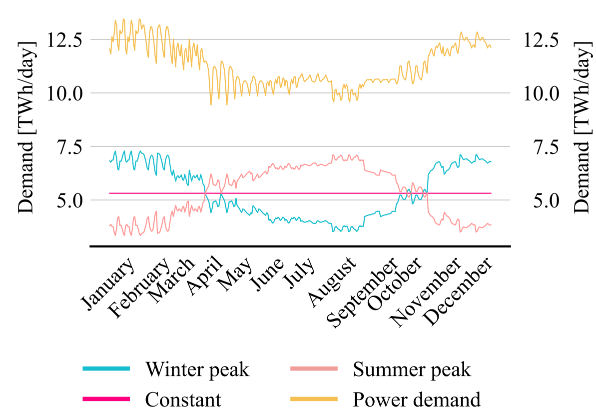

Fig. 3. Comparison of hydrogen and power demand profiles for 2045–2048. These dynamic profiles vary by representative period and are scaled to match annual demand for each investment period.

In summary, the extended EMPIRE framework enables robust analysis of seasonal hydrogen storage by integrating inter-seasonal energy transfer and tactical uncertainty, supporting investment decisions under varying hydrogen demand and operational variability.

4. Case studies and data

This section details the specific model input parameters and case studies used in our analysis.

4.1. Case studies

To address the inherent uncertainty in future hydrogen demand, three distinct seasonal demand profiles are considered: Winter peak, constant, and summer peak. These profiles capture "corners" of the variability in potential hydrogen usage patterns over the year.

The winter peak profile reflects historical natural gas demand, which is higher in winter due to heating, assuming hydrogen may replace natural gas. In contrast, the summer peak profile represents a

Table 3
Key data description and sources.

Data category	Source	Details
Hydrogen demand	[36–39],	Includes profile and flipped demand cases
VRES Power Production	[40,41]	Includes wind, solar, and other renewables
Hydrogen Storage Capacity	Model assumptions, [42]	Includes seasonal storage capacities and cost
Generator Investments	[43]	Includes traditional and renewable generators
Electrolyzer Investments	[44]	Assumed efficiency and cost trends
Operational Costs	Model calculations, [45]	Includes maintenance and variable costs
Geographic Data	Model calculations	20 nodes representing countries and regions in Europe

Table 4
Variable and fixed operational cost sources.

Description	Source
Fixed OM cost for generators	[43]
Variable OM costs for generators	[46]
Fuel costs for generators	[47]
CCS cost time series variable for generators	[48]
Power fixed OM cost for storage	[49]
Energy fixed OM cost for storage	[49]
Storage site fixed OM cost for CO2	[50]
Assumed 5% of CAPEX for CO2 pipeline	[48]
Electrolyzer fixed OM cost for hydrogen	[44]
Assumed 1% of CAPEX for hydrogen pipeline	[51]
Storage fixed OM cost for hydrogen	[52]

reversed pattern, accounting for potential future demand from sectors like heavy-duty transport [35]. The constant profile assumes uniform demand year-round. While actual future demand may differ, these stylized profiles are used to assess how seasonal variation affects the value of hydrogen storage, not to predict demand.

To answer the second research questions from Section 1, the three profiles and their counterparts with seasonal dependence marked with '- *S*' are compared:

1. 'Winter peak' and 'Winter peak - S'
2. 'Constant' and 'Constant - S'
3. 'Summer peak' and 'Summer peak - S'

These six cases are designed to assess how seasonal storage influences investment decisions under different hydrogen demand patterns throughout the year.

In scenarios without seasonal storage, energy levels are not transferred between representative periods. Instead, each period starts and ends with storage at 50% of installed capacity to maintain balance, enforced at each scenario tree node. Fig. 3 shows the hydrogen demand profiles alongside the consistent power demand profile, which peaks in winter.

4.2. Data

EMPIRE minimizes total system costs, categorized by investment and operational costs, all adjusted with a 5% discount rate as per [18]. The cost of investing in increased capacities is aligned with Shirizadeh et al. [3].

EMPIRE models production, transmission, and storage of power and hydrogen, including fossil-based generation with CCS. Key technologies and parameters with sources are summarized in Tables 3 and 4. Initial capacities and cost assumptions are based on publicly available European datasets, which includes cost learning curves for key technologies like renewable generators and electrolyzers. Hydrogen demand is derived from scenario-based projections and historical gas usage patterns, with stochastic sampling preserving correlations with power demand and VRES output. Hydrogen storage investment is modeled as a single investment option per region, potentially including a combination of salt caverns, depleted gas fields, aquifers, and rock caverns. See Appendix B for detailed data sources and assumptions.

4.3. Rolling horizon and multi-stage parameters

The model uses a rolling investment horizon of three periods, with each period lasting three years to align with the EU's green hydrogen additionality rule [7]. The full planning horizon spans eight periods, solved through four overlapping subproblems.

Each investment period includes 12 representative two-week operational periods (336 h each), totaling 4032 hourly-modeled hours. Seasonal variation is captured using monthly partitions. The multi-stage stochastic structure includes three stages per period, with four equally probable branches based on random sampling, split before May and September (see Fig. 1 and Section 3.4).

4.4. Model reproducibility and computational requirements

For reproducibility of the model results, the code and data are available as open access on the public project Github page Hordvei and Hummelen [53]. Running the model requires a Python installation supporting Pyomo [54], and the data is given in Excel-files. In addition, a solver installation is required, e.g., Gurobi. To run the model, execute the python script 'run_EMPIRE.py'.

The numerical instances presented in this paper have been solved on a computer cluster Lenovo ThinkSystem SD530 with 2 × 3.5 GHz Intel Xeon Gold 6144 CPU (8 core) and 384 GB RAM. Solver performance metrics indicate that the average subproblem solution time was approximately 10 h, and four subproblems are solved to roll over the entire horizon ending in 2048. When including the time required for model construction and file operations, the average total solution time, including all subproblems, is 64 h. Furthermore, the maximum memory requirement during execution reached 180 GB.

5. Results and discussion

This section presents and discusses the results, starting with a breakdown of the total system costs and then examining hydrogen and power investment decisions and their operations.

While EMPIRE includes batteries (BESS) and pumped hydro, this study focuses on hydrogen as a seasonal storage option. Batteries are excluded from seasonal storage due to high CAPEX and losses, and pumped hydro is limited by its comparatively small technical potential [55].

5.1. Total system costs

Fig. 4 illustrates the total system costs of the six cases. Among seasonal demand profiles, winter peaks are more expensive than summer peaks. As shown in Fig. 4, without seasonal storage, generator investment costs increase by 2% for summer peaks and 10% for winter peaks compared to constant demand. These higher costs are driven by increased peak demand, with winter peaks requiring more costly infrastructure than summer peaks.

Constant hydrogen demand is generally more cost-effective than seasonal profiles due to better year-round infrastructure utilization. 'Winter peak' scenarios are costlier because the infrastructure needed for high winter demand remains underused in summer. Similarly, 'Summer peak' scenarios require early investments in power generation and

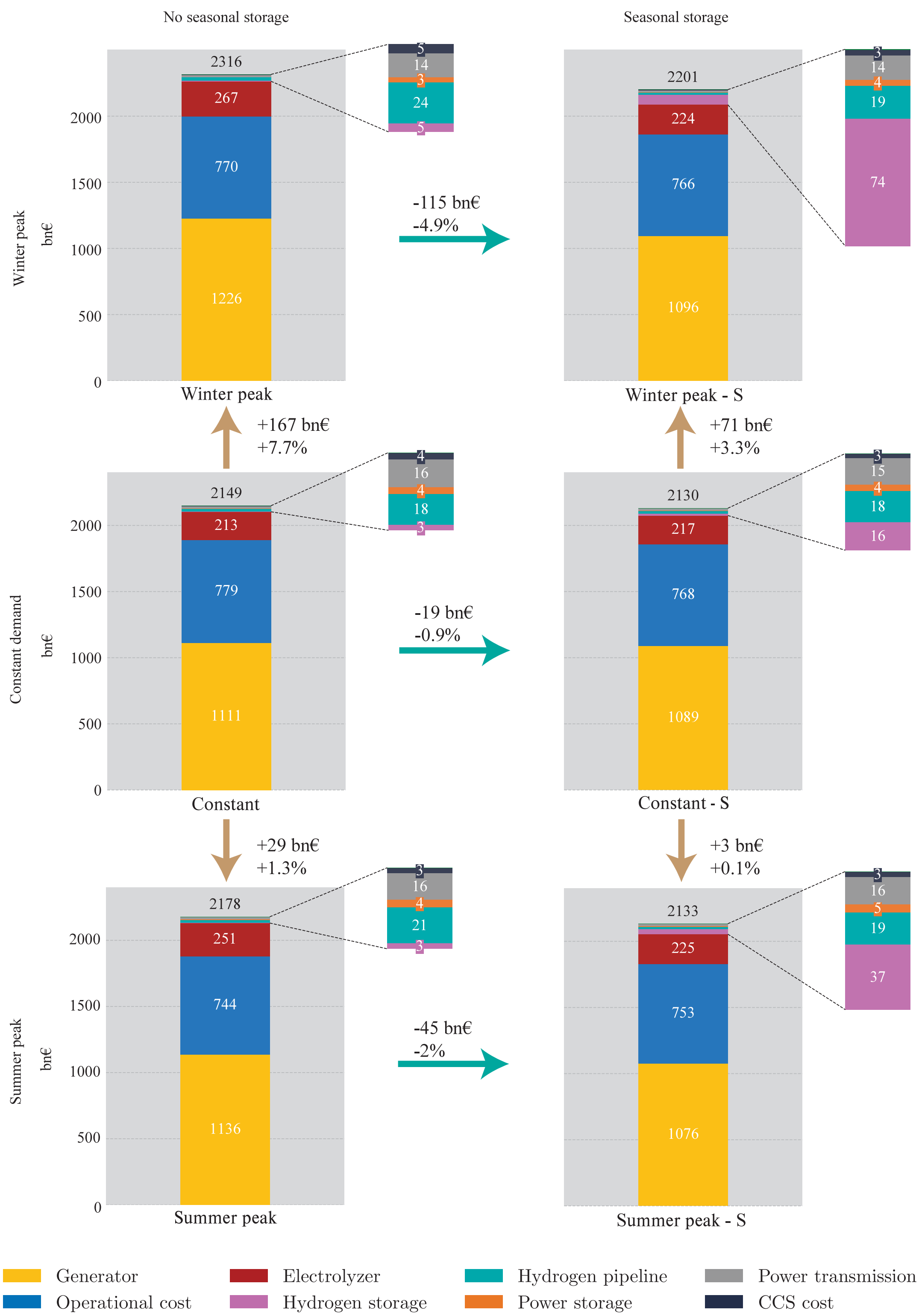

Fig. 4. Total system costs in 2024–2048.

hydrogen pipelines that are underutilized in winter. Although summer peaks align better with solar PV production, the resulting savings are insufficient to offset the higher peak capacity requirements compared to constant demand.

5.2. Cost impact of seasonal hydrogen storage

When seasonal storage is enabled, Fig. 4 shows reduced total system costs for all hydrogen demand profiles, ranging from 1–5% (EUR 19–115 billion) of total system cost, where the highest cost savings result when hydrogen demand peaks in winter. Comparing constant hydrogen demand with seasonal variability reveals that constant demand generally incurs 0–8% (EUR 3–167 billion) lower total system costs, both with and without seasonal hydrogen storage.

Seasonal hydrogen storage reduces total system costs primarily by lowering generator investment, saving EUR 22–130 billion across demand profiles. Although storage investment rises by EUR 13–69 billion, it offsets the need for more costly generation capacity.

In the ‘Winter peak’ case, storing hydrogen from summer for winter use is more cost-effective than ramping up winter electrolyzer production. Without storage, higher winter demand and limited solar output drive up investments in electrolyzers and generators. Seasonal storage offsets these needs, despite added storage costs, leading to significant savings.

In the ‘Summer peak’ case, seasonal hydrogen storage reduces system costs by 2%, despite alignment with solar output in later years (Appendix I). This is due to reduced need for additional generators, electrolyzers, and operational costs. However, ‘Summer peak - S’ is slightly more expensive than ‘Constant - S’ because the need for early investments in storage and electrolyzers to satisfy peak demand during summer means that future technology cost reductions are not captured.

5.3. Hydrogen investments and geographic differences

The increased storage capacities for seasonal hydrogen storage are shown in Fig. 5, which presents geographic differences in expected annual hydrogen production, hydrogen pipelines, and hydrogen storage capacities in 2045.

In general, adding seasonal storage reduces pipeline capacity needs by improving pipeline utilization during low-demand periods. However, under constant hydrogen demand, pipelines are already optimized for steady use, so seasonal storage barely reduces pipeline costs (Fig. 4). Spain sees the largest storage increase from ‘Constant’ to ‘Constant - S’, enabling a 7% reduction in pipeline capacity to France by 2045. However, in the rest of Europe, storage expansion is limited, as constant demand can be efficiently met through consistently utilized pipelines without requiring local storage.

In the ‘Winter peak - S’ scenario, hydrogen storage is most extensive and widely distributed, with Spain, France, and Germany seeing the largest increases. This allows a 12% reduction in pipeline capacity between Spain and France by 2045, as surplus hydrogen can be stored during periods of high production. Locating storage near major demand centers reduces the need for long-distance transmission from Southern to Northern Europe during winter peaks. France plays a key intermediary role due to its central location and borders with several high-demand countries, enabling efficient redistribution of hydrogen and contributing to a 15% reduction in total European pipeline capacity by 2045.

In the transition from ‘Summer peak’ to ‘Summer peak - S’, storage increases are modest and spread across many regions, unlike the concentrated expansions seen in ‘Winter peak - S’ and ‘Constant - S’. This is because summer peak demand aligns with high solar output, reducing the need for seasonal balancing to about half of that in ‘Constant - S’. Additionally, summer storage shifts the spatial distribution of hydrogen production (see Appendix C).

Notably, while hydrogen storage investment costs are higher in ‘Summer peak - S’ than in ‘Constant - S’ (Fig. 4), total storage capacity is lower in 2045. This is due to front-loaded investments in ‘Summer peak - S’, with later investments benefiting from technology learning and lower future costs (see Appendix E).

5.4. Hydrogen system operations

Allowing seasonal storage changes the operational decisions regarding hydrogen production and storage. Fig. 6 shows the expected storage levels, hydrogen production, hydrogen demand met, and hydrogen burnt for power in 2045. The plots display median storage trajectories, as well as the 25th to 75th percentile in the stochastic scenarios.

In all cases without seasonal storage, the expected production profiles closely follow the demand curves. Limited investments in storage necessitate matching production to demand to avoid high load-shedding costs. Conversely, despite differing demand curves, the expected production profiles are similar in all cases with seasonal storage. The introduction of seasonal storage allows for a strategy where all excess VRES production is utilized for hydrogen production, regardless of immediate demand.

Hydrogen will be used for power in non-seasonal storage cases due to the absence of seasonal balancing without seasonal energy storage. This topic will be elaborated further in Appendix G.

5.5. Power generation differences between demand scenarios

Fig. 7 shows power production differences between peaking and constant hydrogen demand cases by presenting aggregated values over six years for clarity and ease of interpretation. Winter-peaking hydrogen demand aligns poorly with solar power, making it a less cost-effective option than constant demand. Consequently, solar generation decreases in winter-peaking scenarios, replaced by power generators better suited to high winter demand, such as wind, biomass, nuclear, hydrogen CCGT, and fossil-based generators.

In contrast, summer peaking hydrogen demand correlates well with seasonal solar production variation, which makes solar a competitive alternative. Consequently, cheap solar replaces expensive investments including fossil-based generators with carbon capture and storage, nuclear, and biomass.

Although annual hydrogen and power demand are exogenous, Fig. 7 mostly show that the power differences above the horizontal zero line are not equal to the part below zero. The majority of these differences result from losses, with smaller amounts of load shedding.

In all cases without seasonal storage, some power comes from burning hydrogen, which is a major loss source. Furthermore, in cases with higher solar production, power is more likely to be transmitted between regions or stored in batteries, causing higher losses.

5.6. Power generation differences with seasonal storage

Fig. 8 shows power production differences between seasonal and non-seasonal storage cases. Seasonal hydrogen storage enhances the value of variable renewable energy sources, particularly solar, by enabling better alignment between production and demand. Seasonal storage reduces the need for installed production capacity, while total power generation remains nearly unchanged until 2042, meaning that utilization of installed capacity is higher with seasonal storage.

Between 2042 and 2048, all seasonal storage scenarios in Fig. 8 show a marked reduction in the use of dispatchable power, as stored hydrogen and increased renewable generation meet a larger share of demand. The largest reduction occurs in the ‘Winter peak’ scenario, where over 600 TWh/year of dispatchable generation is replaced primarily by solar power. In the ‘Constant’ scenario, solar substitutes more than 300 TWh/year, while ‘Summer peak’ reduces excess solar generation and the need to reconvert hydrogen to electricity. Seasonal

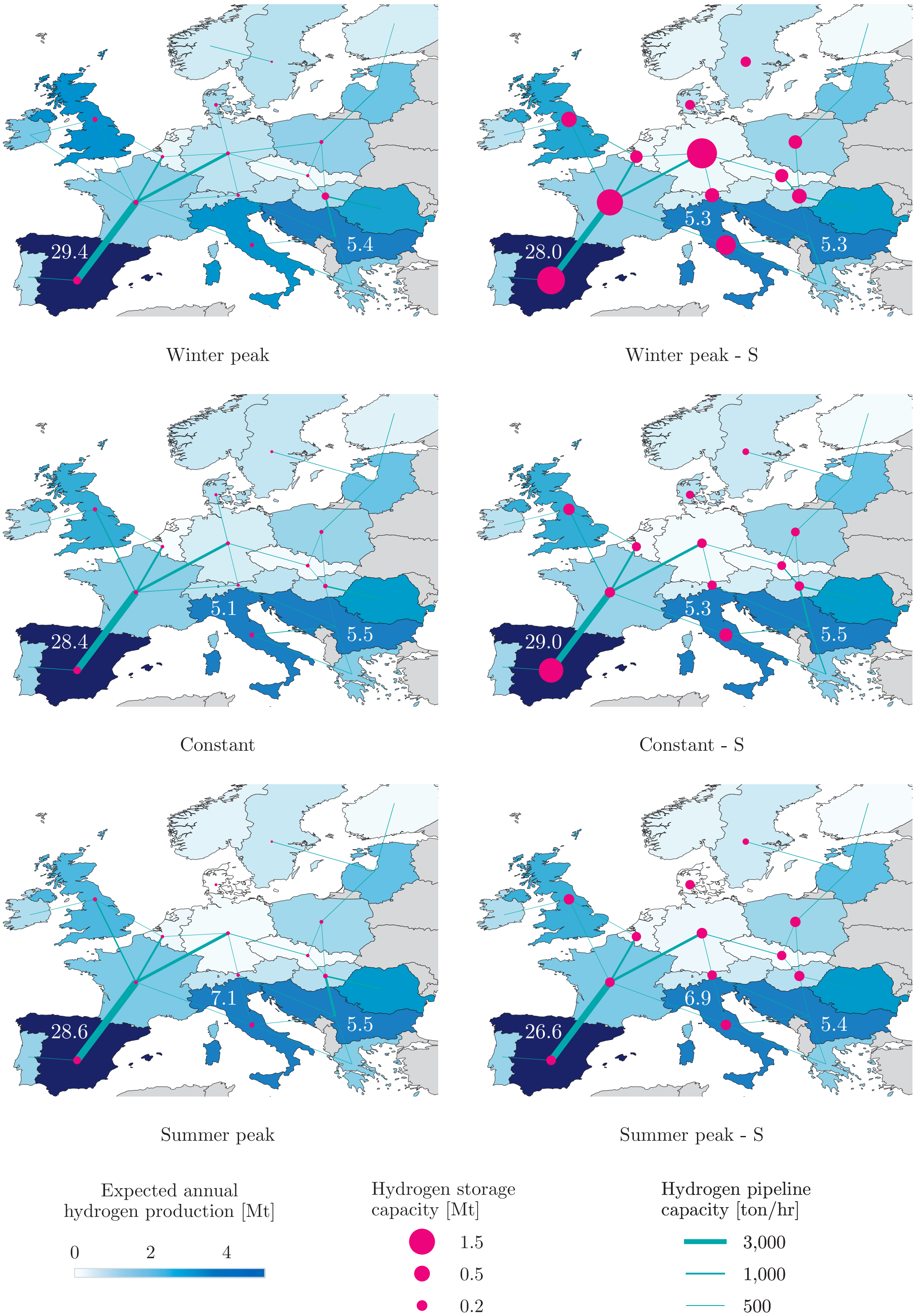

Fig. 5. Expected annual hydrogen production, hydrogen pipelines, and hydrogen storage capacities in 2045. Regions with annual hydrogen production exceeding 5 Mt are plotted as numbers. Pipelines with less than 100 ton/h capacity are not shown.

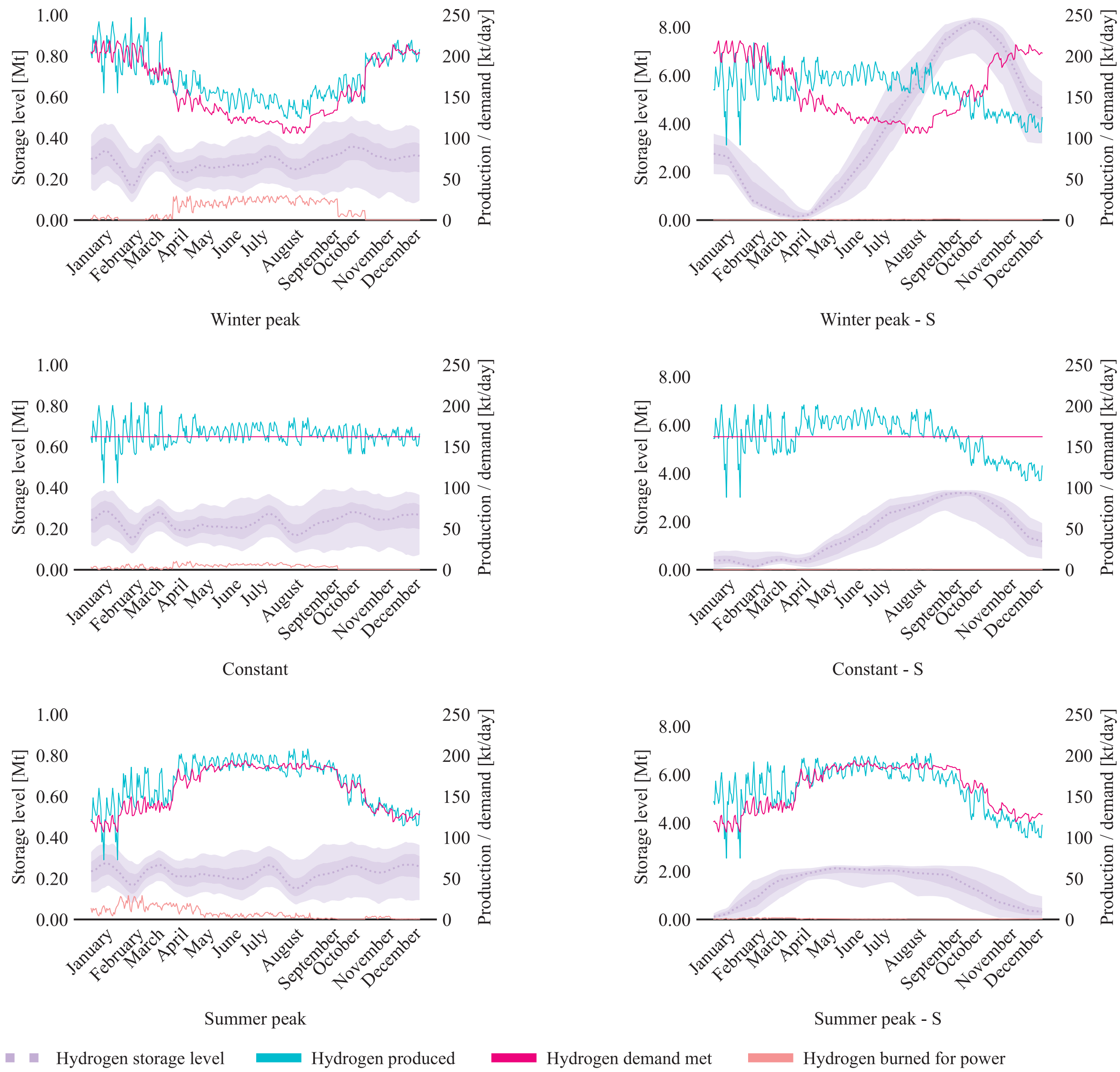

Fig. 6. Annual hydrogen storage, production, and demand profiles in 2045. The median is shown as a dotted line, with shaded areas indicating the interquartile range (25th to 75th percentile).

storage also lowers reliance on infrastructure with high conversion losses, such as long-distance transmission and batteries, resulting in a reduced overall need for power production during this period.

Overall, seasonal storage is advantageous for VRES production due to the ability to store substantial hydrogen produced by non-dispatchable energy sources over a long time. Furthermore, the higher the demand during summer, the more competitive solar production becomes. Note that the average annual difference in solar production between 'Constant' and 'Summer peak' cases of 500 TWh is a relative increase of 4.18%. Thus, the total production mix is relatively similar for all cases, although a clear pattern on what impacts generator investments is seen. Lastly, seasonal storage has a stabilizing effect on seasonal power prices, showing in particular that the median price throughout a year fluctuates considerably less when seasonal storage is allowed. This is discussed in further detail in Appendix F

5.7. Limitations and future research

This study has several limitations that should be considered when interpreting the results. First, future hydrogen demand remains highly uncertain due to hydrogen's emerging role across sectors. The seasonal demand profiles used are illustrative rather than predictive and may not reflect future dynamics, especially if driven by sectors like heavy transport or industry. More detailed sectoral modeling or adaptive demand projections could improve future analyses.

Second, the model assumes a fixed trajectory of technology parameters, such as electrolyzer efficiency and cost. If technological advancements evolve differently, this could shift the balance between production and storage investments. For example, higher electrolyzer efficiency may favor on-demand hydrogen production over seasonal storage. Incorporating learning curves or uncertainty in technology development would better capture these effects.

Third, renewable energy availability is based on random sampling of historical weather data, which may not fully capture future climate uncertainty or extreme events. As climate patterns shift, this approach could underestimate long-term variability. For example, research has already shown changes in hydropower potentials due to climate change [56]. Future work could incorporate advanced meteorological models or synthetic extreme weather years for more robust representation.

Fourth, while hydrogen storage is the focus for seasonal flexibility, other options, such as demand response [57] or power-to-X [58], are

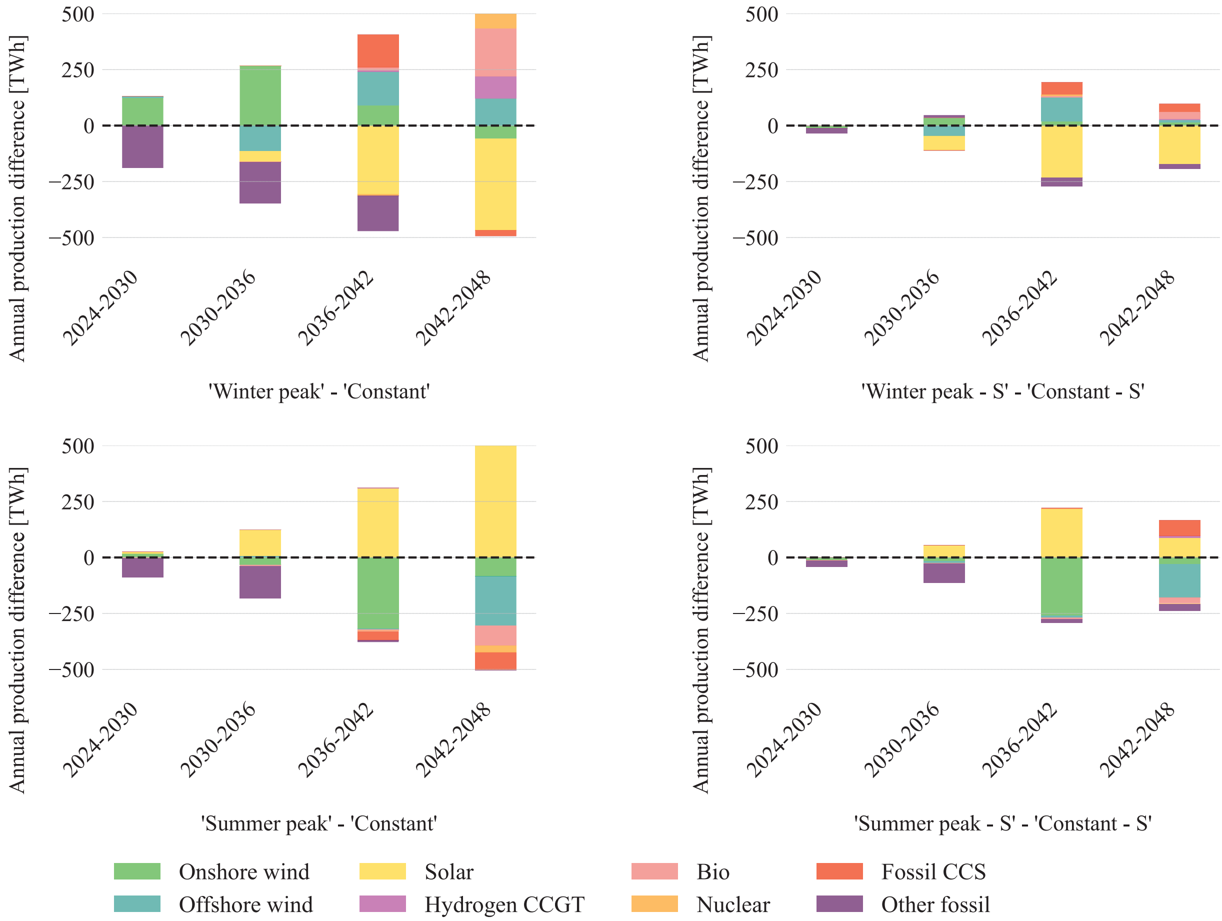

Fig. 7. Power production differences between peaking and constant demand cases.

not fully represented. Including a broader set of flexibility solutions would provide a more comprehensive view of system-wide trade-offs.

Fifth, the spatial resolution is limited to 20 aggregated nodes, which simplifies modeling but may underestimate local transmission bottlenecks and regional variations in supply and demand. This could lead to underestimation of infrastructure needs and misallocation of storage. Higher-resolution or hybrid models could address this.

Sixth, the rolling horizon approach improves computational tractability but may lead to suboptimal, myopic investment decisions due to limited foresight. While this reflects some aspects of real-world decision-making, advanced decomposition methods [19,21] could improve coordination across time steps and enhance solution quality.

Finally, although tactical uncertainty is modeled, the approach still simplifies real-world decision-making by system operators and investors, who respond to evolving market signals, regulations, and risk preferences. Future work could explore more adaptive or behavior-based modeling frameworks to better reflect these complexities.

6. Conclusion

6.1. Concluding remarks

This study extends the EMPIRE model to incorporate tactical uncertainty, enabling a more accurate representation of seasonal hydrogen storage within energy system planning. To address the computational complexity introduced by this enhancement, a rolling horizon approach is employed, allowing for iterative solution of subproblems with reduced temporal scope.

The principal contributions and insights of this work are summarized as follows:

Modeling tactical uncertainty: A novel framework restructures the EMPIRE model to represent seasonal storage in multi-horizon capacity expansion by formulating operational subproblems as multi-stage stochastic programs. This captures tactical uncertainty between representative periods and avoids assuming perfect foresight. A rolling investment horizon ensures computational tractability while maintaining consistency in investment and operational decisions.

Value of seasonal storage: With strong seasonal supply–demand variation, enabling inter-seasonal energy transfer increases hydrogen storage investments by factors of 5–14 and enhances system flexibility, reducing reliance on pipelines and dispatchable generation. It also boosts the value of variable renewables, especially solar, by improving seasonal balancing and infrastructure utilization. The results highlight that ignoring seasonal dynamics can significantly undervalue renewables' potential to replace dispatchable sources.

Implications of seasonal hydrogen demand profiles: Analyzing three hydrogen demand profiles reveals that the European energy system is highly sensitive to seasonal variation. Winter-peaking demand leads to higher production and storage costs

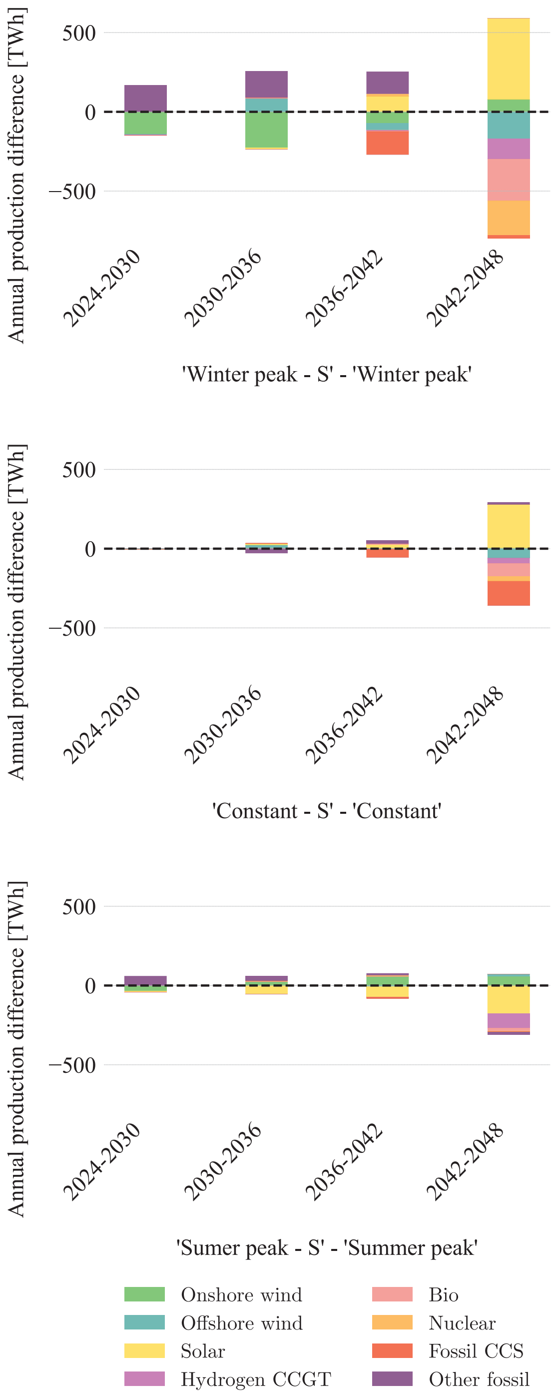

Fig. 8. Power production differences between seasonal and non-seasonal storage cases.

and greater reliance on dispatchable power and wind. Given the uncertainty in future demand patterns, models should account for seasonal variability to ensure robust, cost-effective planning.

6.2. Policy implications

While the model highlights cost-effective storage and transmission strategies, real-world implementation may face policy and regulatory hurdles, such as permitting delays and limited cross-border coordination. Current market structures also undervalue long-duration storage and flexibility. Overcoming these challenges requires proactive policy design, harmonized regulations, and incentives that reward system-wide flexibility. Policymakers should prioritize:

Adaptive investment frameworks: Traditional planning frameworks often overlook the value of flexible infrastructure. Policymakers should adopt frameworks that support phased deployment of hydrogen infrastructure. This is crucial given uncertainties in future hydrogen demand, which is shown in this paper to significantly influence technology choices and regional roles.
Regional coordination for hydrogen infrastructure: Countries like France play a key role as intermediary hubs due to their central location and network connectivity. Strengthening EU-wide coordination can optimize hydrogen flows, storage placement, and cross-border infrastructure planning.
Incentives for flexibility and storage: Seasonal hydrogen storage enhances renewable integration and reduces reliance on dispatchable power. Governments should promote demand-side flexibility and support storage deployment to improve system efficiency and resilience.

6.3. Final remarks

This study demonstrates the importance of integrating tactical uncertainty and seasonal hydrogen storage into long-term energy system planning. By extending the EMPIRE model, we provide a more realistic and flexible framework for evaluating infrastructure investments under uncertainty. The findings emphasize that overlooking seasonal dynamics and uncertainty can lead to suboptimal decisions, under-investment in storage, and over-reliance on dispatchable generation. As Europe moves toward a net-zero energy system, planning tools must evolve to reflect the complexity of future energy systems. This work contributes to that evolution, offering both methodological advancements and actionable insights for researchers, system planners, and policymakers navigating the energy transition.

CRediT authorship contribution statement

Sebastian Emil Hummelen: Conceptualization, Software, Formal analysis, Investigation, Visualization, Methodology, Project administration, Writing – original draft, Writing – review & editing. **Erlend Hordvei:** Conceptualization, Software, Formal analysis, Investigation, Visualization, Methodology, Project administration, Writing – original draft, Writing – review & editing. **Marianne Petersen:** Conceptualization, Supervision, Project administration, Writing – review & editing. **Stian Backe:** Conceptualization, Supervision, Methodology, Writing – review & editing. **Hongyu Zhang:** Supervision, Methodology, Writing – review & editing. **Pedro Crespo del Granado:** Supervision.

Disclosure of use of AI-tools

During the preparation of this work, the authors used ChatGPT and Microsoft CoPilot to improve structure, readability, and language. After using these tools, the authors reviewed and edited the content as needed and takes full responsibility for the content of the publication.

Declaration of competing interest

The authors declare that they have no known competing financial interests or personal relationships that could have appeared to influence the work reported in this paper.

Acknowledgments

This publication has been funded by the Hydrogen Pathways 2050 project - Transition of the Norwegian society and value creation from export (project code 326769) and the NordicH2ubs project - Roadmaps toward 2030 and 2040 (project code 346870). The authors gratefully acknowledge the financial support from the Research Council of Norway and both projects' user partners.

Appendix A. Mathematical formulation

ψ	Operational node
c	Commodity
h	Operational hour
i, j	Investment period
n, m	Geographical node
p	Production method
b	Storage type
t	Transmission type
Ψ	Operational Nodes
$\mathcal{C}$	Commodities
$\mathcal{H}$	Operational hours
$\mathcal{N}$	Geographical nodes
$\mathcal{I}$	Investment periods
$\mathcal{L}_n^c$	All possible bidirectional arcs to node n for commodity c
$\mathcal{P}^c$	Production methods for commodity c
$\mathcal{B}^c$	Storage types for commodity c
$\mathcal{T}^c$	Transmission types for commodity c
σ^c	Sinks of commodity c
$q_{a,i}$	Cost for production, storage, or transmission method a in period i
$q_{n,i}$	Cost for geographical node n in period i
$D^c_{n,h,i,\psi}$	Exogenous demand for commodity c in node n, hour h, period i, scenario ψ
i_p^{life}	Lifetime of production method p
i_t^{life}	Lifetime of transmission type t
i_b^{life}	Lifetime of storage type b
L^{period}	Length of investment periods
$\bar{x}^p_{n,i}$	Remaining initial capacity of production method p in node n, period i
$\bar{x}^b_{n,i}$	Remaining initial capacity of storage type b in node n, period i
$\bar{x}^t_{n,m,i}$	Remaining initial capacity of transmission type t for bidirectional arc (n, m), in period i
α_ψ	Scale factor for operational node ψ
π_ψ	Probability of scenario ψ
r	Annual discount rate
$v^p_{n,i}$	Available capacity of production method p in node n, period i
$v^b_{n,i}$	Available capacity of storage type b in node n, period i
$v^t_{n,m,i}$	Available capacity of transmission type t in bidirectional arc (n, m), period i
$x^p_{n,i}$	Capacity built of production method p in node n, period i
$x^b_{n,i}$	Capacity built of storage type b in node n, period i
$x^t_{n,m,i}$	Capacity built of transmission type t in bidirectional arc (n, m), period i
$y^{c,trans}_{t,n,m,h,i,\psi}$	Transmission at transmission type t for commodity c in bidirectional arc (n, m), hour h, period i, scenario ψ
$y^{c,sink}_{n,h,i,\psi}$	Endogenous demand of commodity c in node n, hour h, period i, scenario ψ
$y^{c,source}_{p,n,h,i,\psi}$	Production of commodity c by production method p in node n, hour h, period i, scenario ψ
$y^{c,ll}_{n,h,i,\psi}$	Load shed of commodity c in node n, hour h, period i, scenario ψ
$y^{c,chrg}_{b,n,h,i,\psi}$	Charging of storage type b for commodity c in node n, hour h, period i, scenario ψ
$y^{c,dischrg}_{b,n,h,i,\psi}$	Discharging of storage type b for commodity c in node n, hour h, period i, scenario ψ
$y^{c,stor}_{b,n,h,i,\psi}$	Storage level of commodity c in storage type b, node n, hour h, period i, scenario ψ

$$\min z = \sum_{i\in\mathcal{I}} (1+r)^{L^{period}(i-1)} \times \Big[\sum_{c\in\mathcal{C}} \Big(\sum_{n\in\mathcal{N}} \sum_{a\in\mathcal{P}^c\cup\mathcal{B}^c} q^{inv}_{a,i} x^a_{n,i} + \sum_{n\in\mathcal{N}} \sum_{m\in\mathcal{L}^c_n} \sum_{t\in\mathcal{T}^c} q^{inv}_{t,i} x^t_{n,m,i}\Big) + v \sum_{\psi\in\Psi} \pi_\psi \sum_{s\in\mathcal{S}} \alpha_\psi \sum_{h\in\mathcal{H}^s} \sum_{n\in\mathcal{N}} \sum_{c\in\mathcal{C}} \sum_{p\in\mathcal{P}^c} q^{operational}_{p,i} y^{c,source}_{p,n,h,i,\psi} + v \sum_{\psi\in\Psi} \pi_\psi \sum_{s\in\mathcal{S}} \alpha_\psi \sum_{h\in\mathcal{H}^s} \sum_{n\in\mathcal{N}} \sum_{c\in\mathcal{C}} q^{c,ll}_{n,i} y^{c,ll}_{n,h,i,\psi}\Big]. \tag{A.1}$$

EMPIRE is a stochastic energy system model aiming at minimizing the total system cost to cover energy demand in Europe. The total system costs include investment costs for production, storage, and transmission, as well as operational costs for production and commodity load shed costs. All costs are discounted with an annual rate r of 5%, where $v = \sum_{j=0}^{(L^{period}-1)} (1+r)^{-j}$ and represents scaling and discounting of the annualized costs to the length of an investment period. The objective function is described in Eq. (A.1).

$$\sum_{p\in\mathcal{P}^c} y^{c,source}_{p,n,h,i,\psi} - \sum_{sink\in\sigma} y^{c,sink}_{n,h,i,\psi} - \sum_{\mathcal{B}^c} (y^{c,chrg}_{b,n,h,i,\psi} - y^{c,dischrg}_{b,n,h,i,\psi}) - \sum_{\mathcal{T}^c} \sum_{m\in\mathcal{L}^c_n} (y^{c,trans}_{t,n,m,h,i,\psi} - y^{c,trans}_{t,m,n,h,i,\psi}) + y^{c,ll}_{n,h,i,\psi} = D^c_{n,h,i,\psi} \tag{A.2}$$

$$\forall\ c\in\mathcal{C},\ n\in\mathcal{N},\ h\in\mathcal{H},\ i\in\mathcal{I},\ \psi\in\Psi.$$

The model is introduced with a general formulation of the flow balance for a commodity c in EMPIRE, covering power and hydrogen. Eq. (A.2) states that the demand of a commodity $D^c_{n,h,i,\psi}$ is to be balanced by the sum of production, endogenous use of commodity, net storage charge, net export, and load shed.

$$y^{c,stor}_{b,n,h,i,\psi} = y^{c,stor}_{b,n,h-1,i,\psi} + y^{c,chrg}_{b,n,h,i,\psi} - y^{c,dischrg}_{b,n,h,i,\psi}, \quad c\in\mathcal{C},\ b\in\mathcal{B}^c,\ n\in\mathcal{N},\ h\in\mathcal{H}_\psi \setminus \mathcal{H}^{Start}_\psi,\ i\in\mathcal{I},\ \psi\in\Psi. \tag{A.3}$$

Table B.5
Maximum hydrogen storage potential by node.

Node	Max capacity [TWh]
Benelux	36
Czech Republic–Slovakia	24
Denmark	3
France	32
Germany	61
Great Britain	5
Hungary	17
Italy	47
Poland	9
Spain	8
Switzerland–Austria	23

Table B.6
Annual hydrogen demand in Mton/year.

Geographic node	2024	2027	2030	2033	2036	2039	2042	2045
Balkan	0.42	0.45	0.48	0.77	1.05	1.33	1.55	1.73
Baltic	0.15	0.17	0.19	0.30	0.41	0.51	0.58	0.63
Benelux	1.44	1.57	1.69	2.58	3.47	4.37	5.35	6.37
Czech Republic–Slovakia	0.27	0.36	0.44	0.76	1.08	1.39	1.62	1.80
Denmark	0.04	0.06	0.08	0.18	0.28	0.38	0.48	0.58
Finland	0.18	0.18	0.18	0.40	0.62	0.85	1.05	1.24
France	0.60	0.67	0.74	1.23	1.72	2.21	2.97	3.86
Germany	1.98	2.33	2.69	5.20	7.71	10.22	11.98	13.36
GreatBrit.	0.80	1.15	1.50	2.85	4.20	5.56	7.21	9.01
Greece	0.33	0.33	0.33	0.43	0.52	0.62	0.75	0.89
Hungary	0.20	0.22	0.24	0.45	0.67	0.88	1.00	1.09
Ireland	0.03	0.06	0.09	0.17	0.26	0.34	0.42	0.49
Italy	0.73	0.92	1.11	2.45	3.80	5.14	5.95	6.49
Norway	0.24	0.36	0.48	0.58	0.68	0.78	0.89	1.01
Poland	0.78	0.78	0.78	1.26	1.74	2.22	2.61	2.95
Portugal	0.11	0.12	0.14	0.23	0.32	0.41	0.51	0.62
Romania	0.17	0.21	0.26	0.54	0.82	1.10	1.30	1.46
Spain	0.61	0.61	0.61	1.17	1.73	2.29	2.86	3.45
Sweden	0.18	0.19	0.20	0.39	0.57	0.76	0.91	1.05
Switzerland-Austria	0.18	0.23	0.29	0.47	0.65	0.82	0.98	1.12
Total	**9.44**	**10.98**	**12.53**	**22.41**	**32.29**	**42.17**	**50.95**	**59.20**

$$y^{c,stor}_{b,n,h,i,\psi} = y^{c,stor,0}_{b,n,h,i,\psi} + y^{c,chrg}_{b,n,h,i,\psi} - y^{c,dischrg}_{b,n,h,i,\psi},$$
$$c \in \mathcal{C},\ b \in \mathcal{B}^c,\ n \in \mathcal{N},\ h = \mathcal{H}^{Start}_{\psi},\ i \in \mathcal{I},\ \psi \in \Psi. \tag{A.4}$$

Eq. (A.3) ensures that, in an operational node ψ, the storage level $y^{c,stor}_{b,n,h,i,\psi}$ at the end of hour h equals to the storage level in the previous hour $y^{c,stor}_{b,n,h-1,i,\psi}$ plus the net charge in the current hour $y^{c,chrg}_{b,n,h,i,\psi} - y^{c,dischrg}_{b,n,h,i,\psi}$. Eq. (A.4) constraints the storage operation in the first hour in each node, where $y^{c,stor,0}_{b,n,h,i,\psi}$ is the initial storage level. These constraints apply to all storage units.

$$y^{c,stor,0}_{b,n,l,i,e} = y^{c,stor,0}_{b,n,h,i,f} + \delta(y^{c,stor}_{b,n,k,i,f} - y^{c,stor,0}_{b,n,h,i,f}),$$
$$c \in \mathcal{C},\ b \in \mathcal{B}^{c,seasonal},\ n \in \mathcal{N}, i \in \mathcal{I},\ e \in \Psi, f \in \Psi_e,$$
$$h \in \mathcal{H}^{Start}_f, k \in \mathcal{H}^{End}_f, l \in \mathcal{H}^{Start}_e. \tag{A.5}$$

Eq. (A.5) ensures that the initial energy storage level in the first operational hour in operational node ψ is passed from the last operational hour in its ancestor node. The Ψ_e is the set of the ancestor node to node e, and δ is the seasonal scaling factor of storage level from one operational node to the next.

$$\sum_{e \in \mathcal{E}} (x^e_{n,i} \times \eta^{PW}_e) \leq \sum_{g \in \mathcal{G}^{VRES}} x^g_{n,i} \qquad \forall\ n \in \mathcal{N},\ i \in \mathcal{I}. \tag{A.6}$$

The additionality constraint, shown in Eq. (A.6), limits electrolyzer investments $x^e_{n,i}$ within the set $\mathcal{E}$ to the generator capacity built $x^g_{n,i}$ within the set of VRES generators $\mathcal{G}^{VRES}$ for each period i and node n. The exogenous parameter η^{PW}_e represents the constant power (PW) consumption for producing one ton of hydrogen (H_2) at electrolyzer e, ensuring that electrolysis power demand does not exceed the capacity of newly built VRES generators.

$$\sum_{e \in \mathcal{E}} (y^{H_2,source}_{e,n,h,i,\psi} \times \eta^{PW}_e) \leq \sum_{g \in \mathcal{G}^{VRES}} (\xi_{g,n,h,i,\psi} \times \sum_{j=i'}^{i} x^g_{n,j})$$
$$\forall\ n \in \mathcal{N},\ i \in \mathcal{I},\ h \in \mathcal{H},\ \psi \in \Psi,\ i' = \max\{1, i - i^{life}_g\}. \tag{A.7}$$

Eq. (A.7) define the spatial and temporal correlation between renewable power generation and electrolysis. Eq. (A.7) limits the hourly power for all electrolysis $\sum_{e \in \mathcal{E}} y^{H_2,source}_{e,n,h,i,\psi}$ to the total available power from additional VRES in that node n and hour h. Parameter $\xi_{g,n,h,i,\psi}$ indicates the stochastic availability of a renewable source, based on historical data, while i^{life}_g accounts for generator depreciation.

$$\sum_{j=i'}^{i} x^p_{n,j} + \bar{x}^p_{n,i} = v^p_{n,i}$$
$$\forall\ c \in \mathcal{C},\ p \in \mathcal{P}^c,\ n \in \mathcal{N},\ i \in \mathcal{I},\ i' = max\{1, i - i^{life}_p\}. \tag{A.8}$$

$$\sum_{j=i'}^{i} x^b_{n,j} + \bar{x}^b_{n,i} = v^b_{n,i}$$
$$\forall\ c \in \mathcal{C},\ b \in \mathcal{B}^c,\ n \in \mathcal{N},\ i \in \mathcal{I},\ i' = max\{1, i - i^{life}_b\}. \tag{A.9}$$

$$\sum_{j=i'}^{i} x^t_{n,m,j} + \bar{x}^t_{n,m,i} = v^t_{n,m,i}$$
$$\forall\ c \in \mathcal{C},\ t \in \mathcal{T}^c,\ n \in \mathcal{N},\ m \in \mathcal{L}^c_n,\ i \in \mathcal{I},\ i' = max\{1, i - i^{life}_t\}. \tag{A.10}$$

Eqs. (A.8)–(A.10) defines the total available capacity of production $v^p_{n,i}$, storage $v^b_{n,i}$ and transmission $v^t_{n,m,i}$ as the sum of all invested capacity within its lifetime. i' represents the first investment period still within the asset's lifetime, relative to the current period i. Total available capacity equals the sum of the invested and initial capacity.

$$y^{c,source}_{p,n,h,i,\psi} \leq v^p_{n,i}$$
$$\forall\ c \in \mathcal{C},\ p \in \mathcal{P}^c,\ n \in \mathcal{N},\ h \in \mathcal{H},\ i \in \mathcal{I},\ \psi \in \Psi. \tag{A.11}$$

$$y^{c,stor}_{b,n,h,i,\psi} \leq v^b_{n,i}$$
$$\forall\ c \in \mathcal{C},\ b \in \mathcal{B}^c,\ n \in \mathcal{N},\ h \in \mathcal{H},\ i \in \mathcal{I},\ \psi \in \Psi. \tag{A.12}$$

$$y^{c,trans}_{t,n,m,h,i,\psi} \leq v^t_{n,i}$$
$$\forall\ c \in \mathcal{C},\ t \in \mathcal{T}^c,\ n \in \mathcal{N},\ m \in \mathcal{L}^c_n,\ h \in \mathcal{H},\ i \in \mathcal{I},\ \psi \in \Psi. \tag{A.13}$$

Eqs. (A.11)–(A.13) assures that assets cannot be operated above the installed capacity.

$$\sum_{s \in \mathcal{S}} \alpha_s \sum_{h \in \mathcal{H}^s} \sum_{n \in \mathcal{N}} \sum_{c \in \mathcal{C}} \sum_{p \in \mathcal{P}^c} \eta^{emission}_p y^{c,source}_{p,n,h,i,\psi} \leq E^{max}_i \qquad \forall\ i \in \mathcal{I},\ \psi \in \Psi. \tag{A.14}$$

Finally, Eq. (A.14) ensures that the total emission in each scenario is limited by the emission cap E^{max}_i for each investment period.

Appendix B. Detailed data sources

The initial power generator and storage capacities are sourced from the European Network of Transmission System Operators for Electricity

Table C.7
Solar capacity factors.

	Solar capacity factor
Spain	16.7%
Portugal	16.6%
Greece	16.0%
Italy	15.3%
Balkan	15.21%

Table C.8
LCOE for solar and wind for selected areas in 2045. Values are not discounted.

	Solar (€/kWh)	Wind (€/kWh)
Spain	0.0321	0.0468
Italy	0.0354	0.0600
Balkan	0.0348	0.0491
Greece	0.0334	0.0456

Table C.9
Modeled distances between selected areas in km.

	Spain	Italy	Balkan
France	920.72	959.64	1595.35
Germany	1725.35	962.83	1262.77
Switzerland	1645.66	524.27	823.90
Poland	2335.06	1404.16	983.84
Benelux	1425.88	1390.70	1690.64

(ENTSO-E) statistical factsheet 2022 [59]. The cost of natural gas is from [45], and the cost of CCS is from [60].

Total hydrogen demand for EU countries is based on the Global Ambition scenario from ENTSO-E [39], while demand for the UK, Switzerland, Norway is sourced from Government [38], AXPO [36], and DNV [37], respectively. Annual hydrogen demand can be seen in Table B.6. Future demand profiles follow historical natural gas patterns from the ENAGAS database [61], using 2015–2019 daily profiles. Where available, industry-specific data is used; otherwise, total demand profiles are applied. Aggregated regions adopt the profile of the largest gas-consuming country, and Norway uses Denmark's profile. Hydrogen demand is sampled alongside other stochastic data to preserve cross-correlations with power demand and VRES output (see Section 3.4). No assumptions are made about specific end-use sectors, though European Network of Transmission System Operators for Electricity (ENTSO-E) [62] note likely dominance by hard-to-abate sectors and synthetic fuel production.

Hydrogen storage capacity and cost data are sourced from Cihlar et al. [42]. The model allows investment in all storage types listed in Table 3 in [42], with a weighted average capital cost of 25.12 EUR/kg hydrogen, covering salt caverns, depleted gas fields, aquifers, and rock caverns. The maximum capacity for development of hydrogen storage is shown in Table B.5.

Appendix C. Why Spain is a dominant hydrogen producer

Table C.7 lists the top five countries with the highest solar capacity factors, calculated as annual output divided by the theoretical maximum at full availability. These values, analogous to Levelized Cost of Energy (LCOE), indicate that Spain offers the lowest-cost solar power, as confirmed in Table C.8. However, the small differences between Spain, Portugal, and Greece suggest that cost alone does not explain Spain's dominance.

Table C.9 shows distances between major producers and consumers. Spain is only marginally closer to France than Italy (by 4%), and not significantly closer to other major consumers, indicating that geographic proximity is not Spain's main advantage.

The final factor influencing a country's competitiveness is year-round availability. While hourly solar peaks are similar across countries, seasonal variation differs significantly. As shown in Fig. C.9, Spain has the most consistent solar output throughout the year, with January and December production reaching 67% and 50% of peak monthly output, respectively. Since hydrogen and electricity demand are highest in winter under the constant and winter peak scenarios, Spain's relatively stable winter production gives it a distinct advantage over other countries.

Lastly, wind production increases in Greece and the Balkans during winter, boosting hydrogen output. However, wind has a higher levelized cost of electricity (LCOE) than solar (Table C.8) and is more valuable for covering evening power demand when solar is unavailable. Solar remains the more economical choice for hydrogen production due to its lower cost and the relative affordability of hydrogen storage.

Appendix D. Hydrogen-solar correlation

Hydrogen production share of Spain in 2045 ranges from 45.0% in the lowest to 49.6% in the highest cases. Furthermore, shares of the whole of southern Europe lay in the range of 65%–70%, demonstrating that solar rich countries produce a majority of hydrogen. The hourly correlation of hydrogen and solar production for Spain in the Winter peak case is displayed in Fig. D.10, showing that hydrogen production will completely shut down when there is no solar production in June, and run at a very low capacity at night during December.

Appendix E. Hydrogen storage investments in cases with seasonal storage

As shown in Section 5.1, hydrogen storage costs are significantly higher in the 'Summer peak - S' scenario compared to 'Constant - S', despite lower total storage in the final period. Fig. E.11 illustrates that 'Summer peak - S' sees substantial early investment in storage compared to 'Constant - S'. Since total costs are expressed in net present value, delayed investments appear cheaper due to technological developments, even if total capacity is higher.

The high initial storage investment in 'Summer peak - S', despite seasonal alignment with solar production, is due to:

High electrolyzer costs early on: Although annual demand is equal across scenarios, 'Summer peak - S' has 20% higher peak days. Given that electrolyzer costs drop by 52% by the final period (pre-discounting), it is more cost-effective to store surplus hydrogen from low-demand days than to oversize electrolyzers for short-lived peaks.

Uncertain demand-supply mismatch: In the constant demand case, future hydrogen needs constant, allowing precise storage planning. In contrast, dynamic profiles require larger storage buffers to hedge against simultaneous demand spikes and low VRES output.

In later periods, 'Summer peak - S' shows reduced storage needs due to better alignment between solar generation and hydrogen demand, along with cheaper electrolyzers. Early reliance on storage to manage summer peaks results in hydrogen production that closely follows surplus VRES availability, as seen in Fig. 6.

Appendix F. Power price distribution

Fig. F.12 shows power shadow prices across scenarios. Unlike actual prices, shadow prices reflect the cost impact of reducing demand by one unit in a given hour. Though demand is perfectly inelastic, making shadow prices more volatile, they still offer insight into future price trends. Seasonal storage helps stabilize these prices: median values (red line) stay within 30% of 50 EUR/MWh year-round, while non-seasonal cases show greater winter variability. Although box heights (price spread) are not smaller with seasonal storage, average prices remain more consistent across seasons.

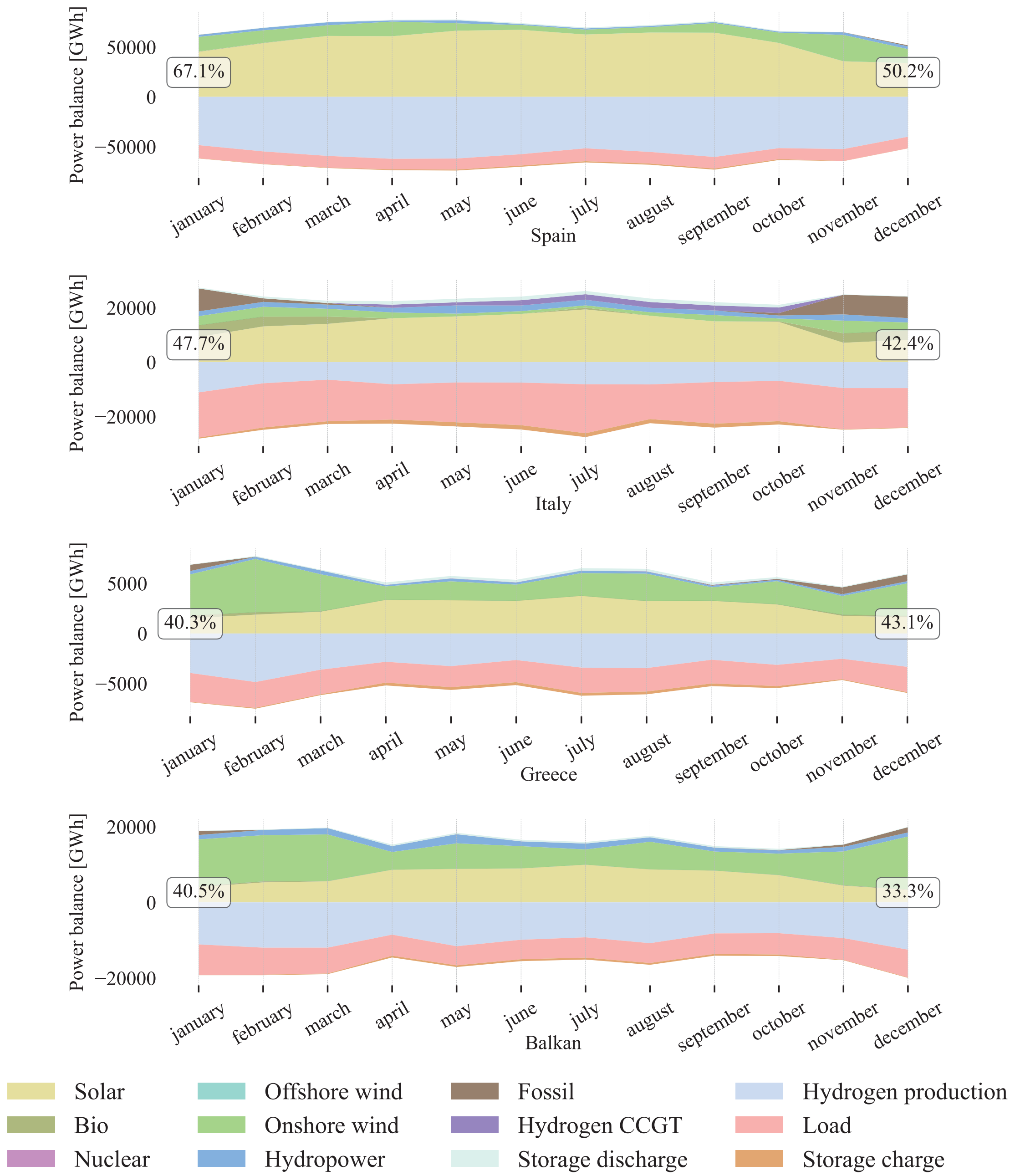

Fig. C.9. Seasonal power balance of Southern European locations in 2045 for the Winter peak case. The percentages for January and December (months with the lowest solar production on average) signify the production ratios for solar output between those months and the maximum producing month.

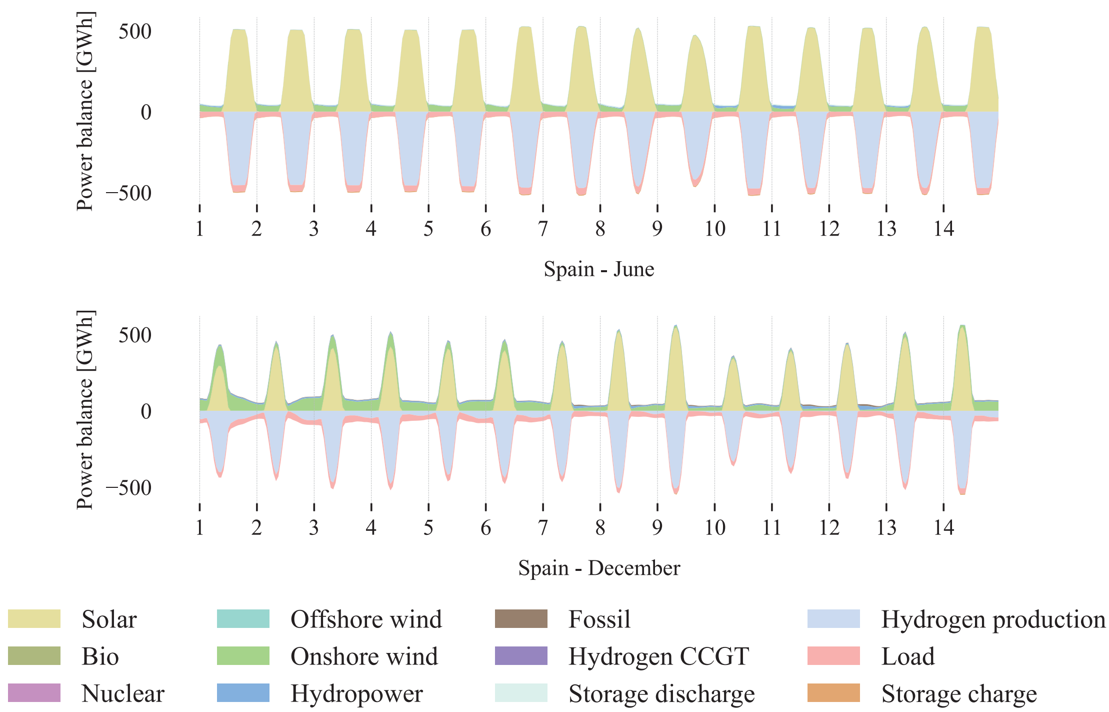

Fig. D.10. Solar-Hydrogen correlation for Spain in June and December 2045 in 'Winter peak - S'.

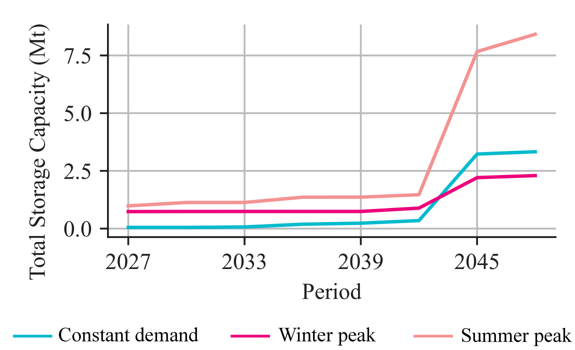

Fig. E.11. Total storage capacity development for seasonal storage cases.

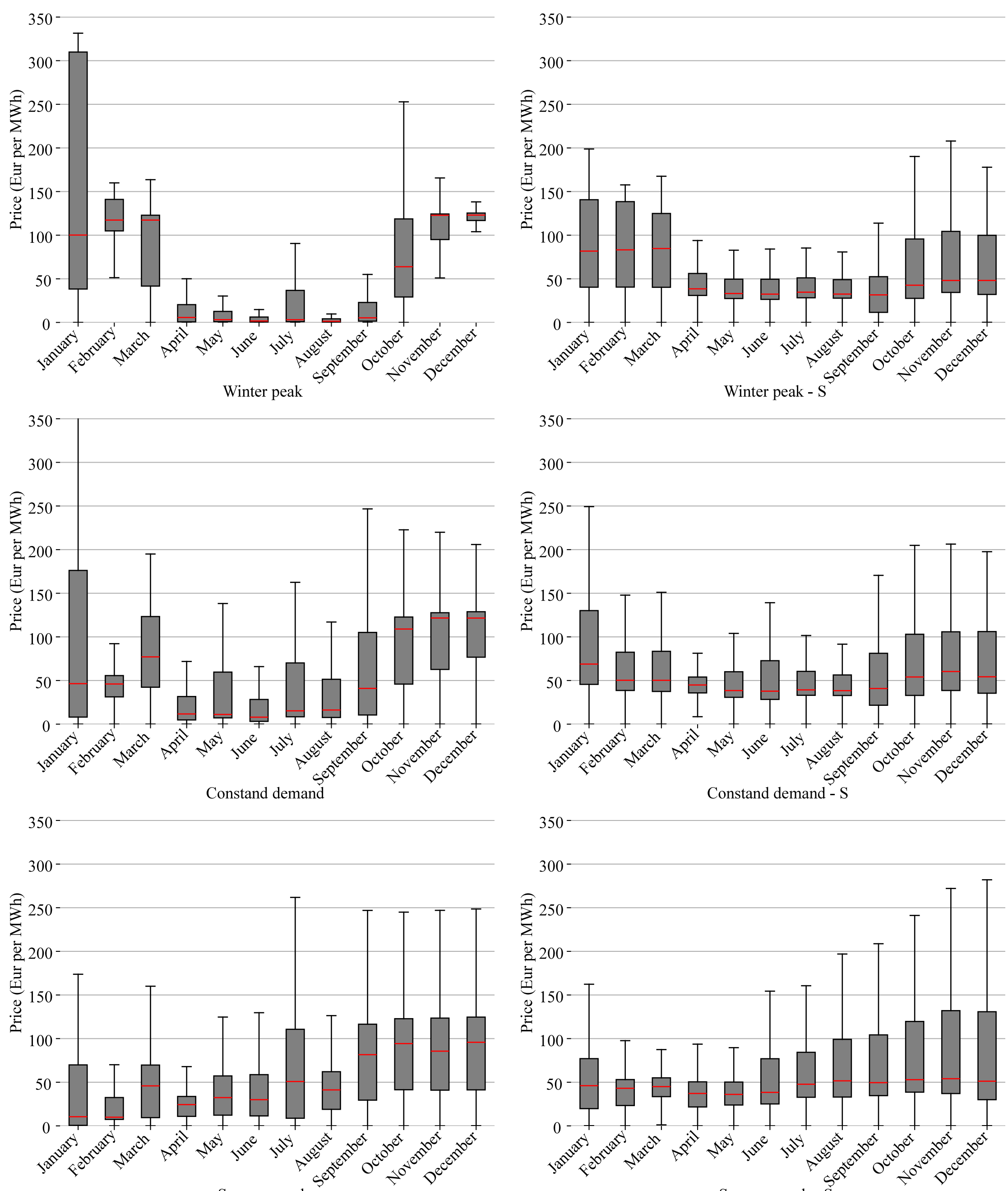

Fig. F.12. Boxplots of power shadow prices for different cases in 2045.

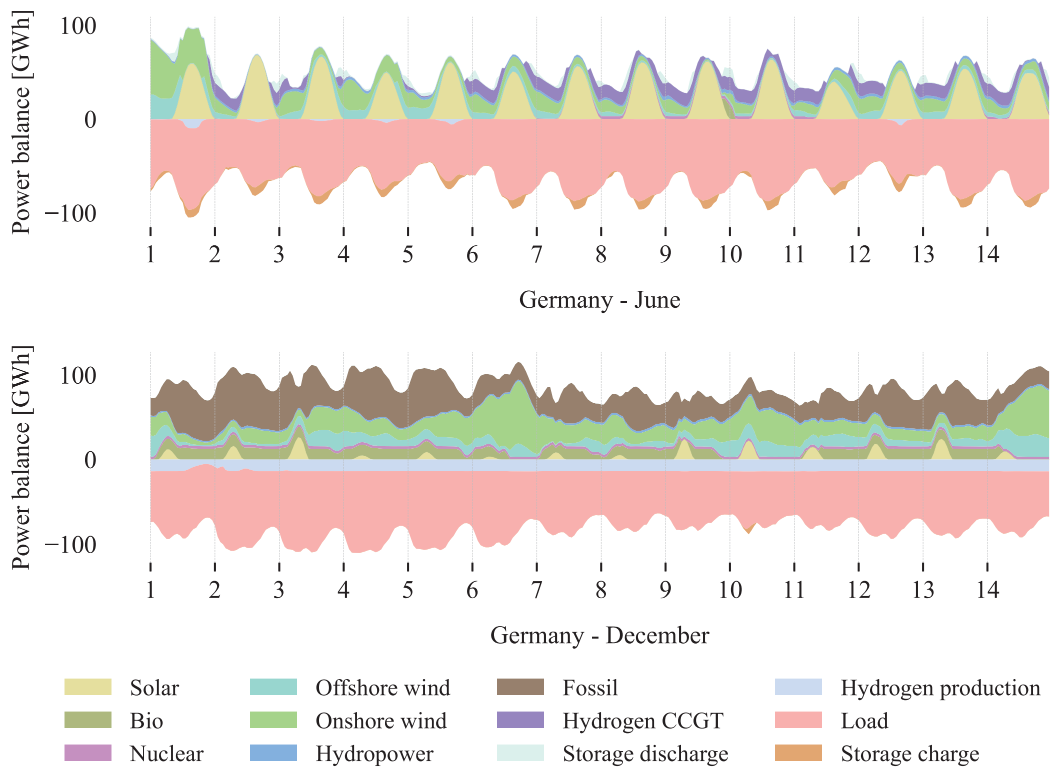

Fig. G.13. Operating plots for Germany in June and December 2045 in 'Winter peak'.

Appendix G. Hydrogen for power

Fig. 6 shows that in all scenarios without seasonal storage, hydrogen is used for power generation despite its low round-trip efficiency (33%–38% [43]). Since hydrogen demand must be met within two weeks each month, systems are sized for peak months, leading to overcapacity during low-demand periods. For instance, in 'Winter peak - S', December requires enough hydrogen and power capacity to meet high demand, while in July, lower demand and higher solar output result in excess hydrogen production, which is stored and used at night as a cheaper alternative to other dispatchable sources. Fig. G.13 illustrates how Germany, the main hydrogen consumer for power in 2045, uses hydrogen to meet night-time power demand when wind power is insufficient.

Appendix H. Spatial aggregation in this EMPIRE version

To manage model complexity, we reduced spatial resolution to 20 European nodes. Smaller or less impactful countries with similar profiles, including the Benelux, Baltics, Balkans, Austria–Switzerland, and Czechia–Slovakia—were aggregated. In contrast, Ireland, the UK, Portugal, and Spain remained separate due to distinct production profiles and significant hydrogen and power roles. Aggregation involved summing demands and capacities, using the dominant country's stochastic profile to preserve realism.

Appendix I. Regional power production and transmission network

See Fig. I.14.

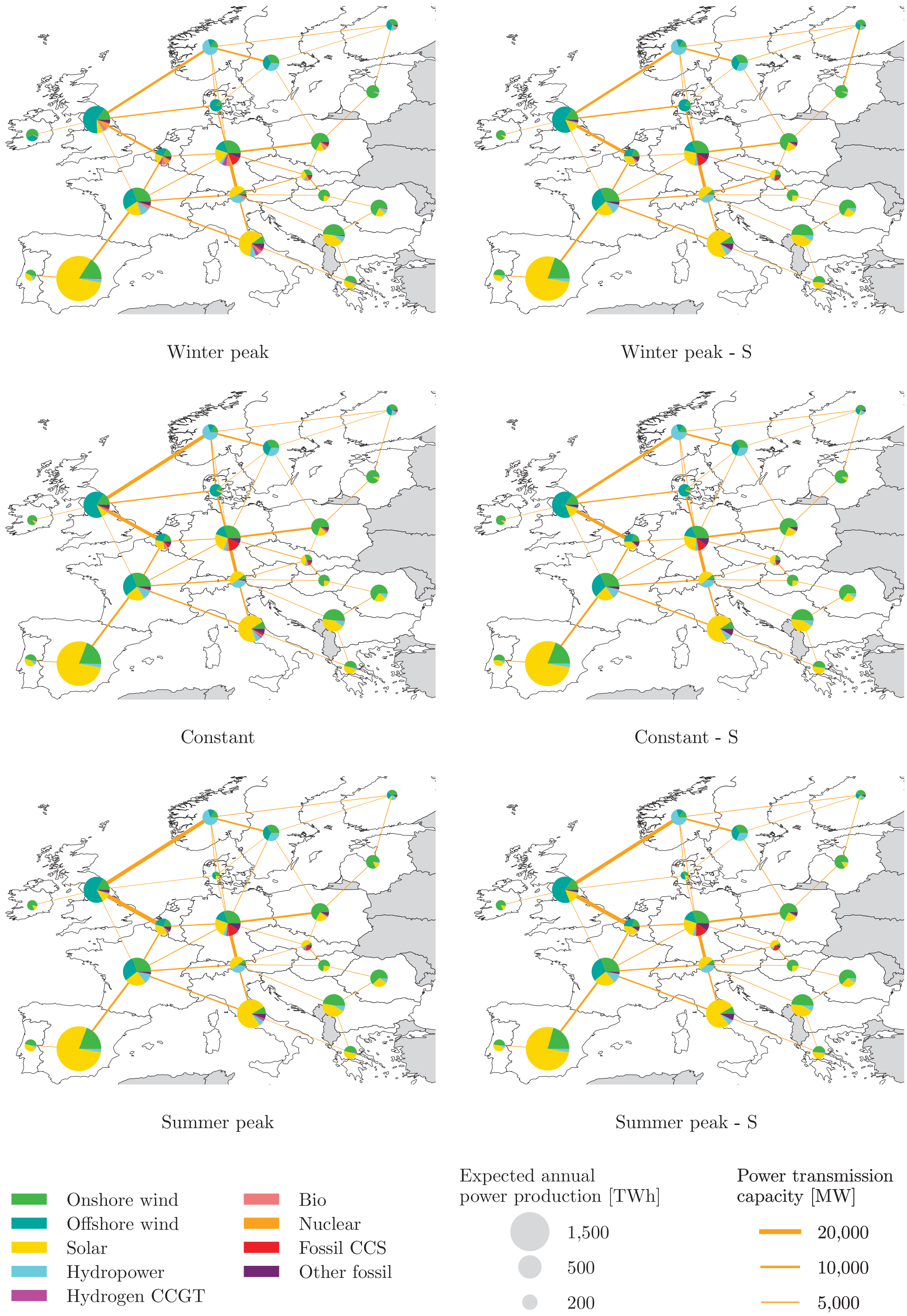

Fig. I.14. Expected annual power production per region and power transmission capacities in 2045.

Data availability

Data will be made available on request.

References

[1] N.V. Sahinidis, Optimization under uncertainty: State-of-the-art and opportunities, Comput. Chem. Eng. 28 (6–7) (2004) 971–983, http://dx.doi.org/10.1016/j.compchemeng.2003.09.017.

[2] G. Schmidt, W.E. Wilhelm, Strategic, tactical and operational decisions in multi-national logistics networks: A review and discussion of modelling issues, Int. J. Prod. Res. 38 (7) (2000) 1501–1523, http://dx.doi.org/10.1080/002075400188690.

[3] B. Shirizadeh, G. Seck, M. Venugopal, E. Hache, M. Villavicencio, S. Douguet, S. Saunier, F. Lagrange, L.-M. Malbec, V. D'Herbemont, J. Straus, G. Reigstad, Hydrogen 4 EU (Hydrogen for Europe report) - Charting pathways to enable net zero - 2022 Edition, 2022, http://dx.doi.org/10.13140/RG.2.2.25307.03367.

[4] A. Buttler, H. Spliethoff, Current status of water electrolysis for energy storage, grid balancing and sector coupling via power-to-gas and power-to-liquids: A review, Renew. Sustain. Energy Rev. (ISSN: 1364-0321) 82 (2018) 2440–2454, http://dx.doi.org/10.1016/j.rser.2017.09.003.

[5] J. Mitali, S. Dhinakaran, A. Mohamad, Energy storage systems: A review, Energy Storage Sav. 1 (3) (2022) 166–216, http://dx.doi.org/10.1016/j.enss.2022.07.002.

[6] M. Jafari, M. Korpås, A. Botterud, Power system decarbonization: Impacts of energy storage duration and interannual renewables variability, Renew. Energy 156 (2020) 1171–1185, http://dx.doi.org/10.1016/j.renene.2020.04.144.

[7] E. Hordvei, S.E. Hummelen, M. Petersen, S. Backe, P.C. del Granado, From policy to practice: Upper bound cost estimates of Europe's green hydrogen ambitions, Cleaner Energy Systems (2025) 100206, http://dx.doi.org/10.1016/j.cles.2025.100206.

[8] F. Neumann, E. Zeyen, M. Victoria, T. Brown, The potential role of a hydrogen network in europe, Joule 7 (8) (2023) 1793–1817, http://dx.doi.org/10.1016/j.joule.2023.06.016.

[9] I. Kountouris, R. Bramstoft, T. Madsen, J. Bermúdez, M. Münster, D. Keles, A unified European hydrogen infrastructure planning to support the rapid scale-up of hydrogen production, 2023, http://dx.doi.org/10.21203/rs.3.rs-3185467/v1, Preprint (Version 1) available at Research Square.

[10] P. Gabrielli, A. Poluzzi, G.J. Kramer, C. Spiers, M. Mazzotti, M. Gazzani, Seasonal energy storage for zero-emissions multi-energy systems via underground hydrogen storage, Renew. Sustain. Energy Rev. 121 (2020) 109629, http://dx.doi.org/10.1016/j.rser.2019.109629.

[11] L.S. Strømholm, R.A.S. Rolfsen, Flexible Hydrogen Production: A Comprehensive Study on Optimizing Cost-Efficient Combinations of Production and Storage Capacity to Exploit Electricity Price Fluctuations (Master thesis), Norwegian School of Economics, Bergen, 2021, URL: https://openaccess.nhh.no/nhh-xmlui/bitstream/handle/11250/2770501/masterthesis.pdf?sequence=1.

[12] M. Kaut, Handling of long-term storage in multi-horizon stochastic programs, Comput. Manag. Sci. 21 (1) (2024) 1–26, http://dx.doi.org/10.1007/s10287-024-00508-z.

[13] L. Zhang, C. Jia, F. Bai, W. Wang, S. An, K. Zhao, Z. Li, J. Li, H. Sun, A comprehensive review of the promising clean energy carrier: Hydrogen production, transportation, storage, and utilization (HPTSU) technologies, Fuel 355 (2024) 129455, http://dx.doi.org/10.1016/j.fuel.2023.129455.

[14] P. Martin, I.B. Ocko, S. Esquivel-Elizondo, R. Kupers, D. Cebon, T. Baxter, S.P. Hamburg, A review of challenges with using the natural gas system for hydrogen, Energy Sci. Eng. 12 (10) (2024) 3995–4009, http://dx.doi.org/10.1002/ese3.1861.

[15] H. Majidi, M.M. Hayati, C. Breyer, B. Mohammadi-ivatloo, S. Honkapuro, H. Karjunen, P. Laaksonen, V. Sihvonen, Overview of energy modeling requirements and tools for future smart energy systems, Renew. Sustain. Energy Rev. 212 (2025) 115367, http://dx.doi.org/10.1016/j.rser.2025.115367.

[16] H. Abgottspon, G. Andersson, Medium-term optimization of pumped hydro storage with stochastic intrastage subproblems, in: 2014 Power Systems Computation Conference, 2014, pp. 1–7, http://dx.doi.org/10.1109/PSCC.2014.7038352.

[17] G. Durakovic, H. Zhang, B.R. Knudsen, A. Tomasgard, P.C. del Granado, Decarbonizing the European energy system in the absence of Russian gas: Hydrogen uptake and carbon capture developments in the power, heat and industry sectors, J. Clean. Prod. (ISSN: 0959-6526) 435 (2024) 140473, http://dx.doi.org/10.1016/j.jclepro.2023.140473.

[18] S. Backe, C. Skar, P.C. Del Granado, O. Turgut, A. Tomasgard, EMPIRE: An open-source model based on multi-horizon programming for energy transition analyses, SoftwareX 17 (2022) 100877, http://dx.doi.org/10.1016/j.softx.2021.100877.

[19] H. Zhang, I.E. Grossmann, K. McKinnon, B.R. Knudsen, R.G. Nava, A. Tomasgard, Integrated investment, retrofit and abandonment energy system planning with multi-timescale uncertainty using stabilised adaptive benders decomposition, European J. Oper. Res. (ISSN: 0377-2217) 325 (2) (2025) 261–280, http://dx.doi.org/10.1016/j.ejor.2025.04.005.

[20] H. Zhang, N. Mazzi, K. McKinnon, R.G. Nava, A. Tomasgard, A stabilised benders decomposition with adaptive oracles for large-scale stochastic programming with short-term and long-term uncertainty, Comput. Oper. Res. (ISSN: 0305-0548) 167 (2024) 106665, http://dx.doi.org/10.1016/J.COR.2024.106665.

[21] H. Zhang, I.E. Grossmann, A. Tomasgard, Decomposition methods for multi-horizon stochastic programming, Comput. Manag. Sci. 2024 21: 1 (ISSN: 1619-6988) 21 (1) (2024) 1–24, http://dx.doi.org/10.1007/S10287-024-00509-Y.

[22] J. Bistline, W. Cole, G. Damato, J. DeCarolis, W. Frazier, V. Linga, C. Marcy, C. Namovicz, K. Podkaminer, R. Sims, et al., Energy storage in long-term system models: A review of considerations, best practices, and research needs, Prog. Energy 2 (3) (2020) 032001, http://dx.doi.org/10.1088/2516-1083/ab9894.

[23] R. Sioshansi, P. Denholm, J. Arteaga, S. Awara, S. Bhattacharjee, A. Botterud, W. Cole, A. Cortes, A. De Queiroz, J. DeCarolis, et al., Energy-storage modeling: State-of-the-art and future research directions, IEEE Trans. Power Syst. 37 (2) (2021) 860–875, http://dx.doi.org/10.1109/TPWRS.2021.3104768.

[24] A.M. Elberry, J. Thakur, J. Veysey, Seasonal hydrogen storage for sustainable renewable energy integration in the electricity sector: A case study of Finland, J. Energy Storage 44 (2021) 103474, http://dx.doi.org/10.1016/j.est.2021.103474.

[25] Y.-S. Fu, I.-Y.L. Hsieh, Evaluating the feasibility and economics of hydrogen storage in large-scale renewable deployment for decarbonization, Energy Strat. Rev. (ISSN: 2211-467X) 55 (2024) 101545, http://dx.doi.org/10.1016/j.esr.2024.101545.

[26] E. Sahraie, I. Kamwa, A. Moeini, S.M. Mohseni-Bonab, Techno-economic synergy analysis of integrated electric power and hydrogen system, Energy Strat. Rev. (ISSN: 2211-467X) 55 (2024) 101515, http://dx.doi.org/10.1016/j.esr.2024.101515.

[27] B. Lux, M. Frömel, G. Resch, F. Hasengst, F. Sensfuß, Effects of different renewable electricity diffusion paths and restricted european cooperation on Europe's hydrogen supply, Energy Strat. Rev. (ISSN: 2211-467X) 56 (2024) 101589, http://dx.doi.org/10.1016/j.esr.2024.101589.

[28] European Commission, A hydrogen strategy for a climate-neutral Europe, 2020.

[29] European Commission, Renewable hydrogen production: New rules formally adopted, 2023, URL: https://energy.ec.europa.eu/news/renewable-hydrogen-production-new-rules-formally-adopted-2023-06-20_en. (Accessed 12 August 2025).

[30] S. Backe, M. Ahang, A. Tomasgard, Stable stochastic capacity expansion with variable renewables: Comparing moment matching and stratified scenario generation sampling, Appl. Energy 302 (2021) 117538, http://dx.doi.org/10.1016/j.apenergy.2021.117538.

[31] S. Backe, M. Korpås, A. Tomasgard, Heat and electric vehicle flexibility in the European power system: A case study of norwegian energy communities, Int. J. Electr. Power Energy Syst. 125 (2021) 106479, http://dx.doi.org/10.1016/j.ijepes.2020.106479.

[32] J. Silvente, G.M. Kopanos, E.N. Pistikopoulos, A. Espuña, A rolling horizon optimization framework for the simultaneous energy supply and demand planning in microgrids, Appl. Energy (ISSN: 0306-2619) 155 (2015) 485–501, http://dx.doi.org/10.1016/j.apenergy.2015.05.090.

[33] K.J. Laverty, Economic "short-termism": The debate, the unresolved issues, and the implications for management practice and research, Acad. Manag. Rev. 21 (3) (1996) 825–860, http://dx.doi.org/10.5465/amr.1996.9702100316.

[34] S. Babrowski, T. Heffels, P. Jochem, W. Fichtner, Reducing computing time of energy system models by a myopic approach: A case study based on the PERSEUS-NET model, Energy Syst. 5 (2014) 65–83, http://dx.doi.org/10.1007/s12667-013-0085-1.

[35] M. de las Nieves Camacho, D. Jurburg, M. Tanco, Hydrogen fuel cell heavy-duty trucks: Review of main research topics, Int. J. Hydrog. Energy 47 (68) (2022) 29505–29525, http://dx.doi.org/10.1016/j.ijhydene.2022.06.271.

[36] AXPO, Rolle und potenzial von wasserstoff in der schweiz, 2023, URL: https://www.axpo.com/ch/en/newsroom/media-releases/2023/hydrogen-energy-crucial-to-a-climate-neutral-future.html.

[37] DNV, Energy transition Norway 2022, 2022, URL: https://www.dnv.com/publications/energy-transition-norway-2022-235535/.

[38] U. Government, UK hydrogen strategy, 2023, URL: https://www.gov.uk/government/publications/uk-hydrogen-strategy/uk-hydrogen-strategy-accessible-html-version.

[39] ENTSO-E, Ten-year network development plan (TYNDP) 2022, 2022, URL: https://tyndp.entsoe.eu/resources/tyndp-2022-2.

[40] S. Pfenninger, Long-term patterns of European PV output using 30 years of validated hourly reanalysis and satellite data, Energy (ISSN: 0360-5442) 114 (2016) 1251–1265, http://dx.doi.org/10.1016/j.energy.2016.08.060.

[41] I. Staffell, S. Pfenninger, Using bias-corrected reanalysis to simulate current and future wind power output, Energy (ISSN: 0360-5442) 114 (2016) 1224–1239, http://dx.doi.org/10.1016/j.energy.2016.08.068.

[42] J. Cihlar, D. Mavins, K. van der Leun, Picturing the value of underground gas storage to the European hydrogen system, 2021, Gas Infrastructure Europe. URL: https://www.gie.eu/gie-presents-new-study-picturing-the-value-of-underground-gas-storage-to-the-european-hydrogen-system/.

[43] ASSET, Technology Pathways in Decarbonisation Scenarios 2018, 2018, URL: https://energy.ec.europa.eu/document/download/c5dac2fb-4682-4795-a1b1-13f8806c9ea8_en?filename=2018_06_27_technology_pathways_-_finalreportmain2.pdf.

[44] D.E. Agency, Cost and Performance Data for Offshore Hydrogen Production, Technical Report, Danish Energy Agency, 2023, URL: https://www.dnv.com/. Assisted by DNV.

[45] European Commission, EU reference scenario 2020, 2020, https://energy.ec.europa.eu/data-and-analysis/energy-modelling/eu-reference-scenario-2020_en.

[46] International Energy Agency, Nuclear Energy Agency, Projected Costs of Generating Electricity 2020, OECD Publishing, Paris, 2020, URL: https://www.iea.org/reports/projected-costs-of-generating-electricity-2020. (Accessed 12 August 2025).

[47] P. Capros, A. De Vita, N. Tasios, P. Siskos, M. Kannavou, A. Petropoulos, S. Evangelopoulou, M. Zampara, D. Papadopoulos, C. Nakos, L. Paroussos, K. Fragiadakis, S. Tsani, P. Karkatsoulis, P. Fragkos, N. Kouvaritakis, L. Höglund-Isaksson, W. Winiwarter, P. Purohit, A. Gomez-Sanabria, S. Frank, N. Forsell, M. Gusti, P. Havlík, M. Obersteiner, H.-P. Witzke, M. Kesting, EU Reference Scenario 2016: Energy, Transport and GHG Emissions Trends to 2050, Publications Office of the European Union, Luxembourg, 2016, http://dx.doi.org/10.2833/001137.

[48] Zero Emissions Platform (ZEP), The costs of CO2 capture, transport and storage, 2011, URL: https://www.zeroemissionsplatform.eu/library/publication/166-zep-cost-report-capture.html. Prepared on behalf of the Advisory Council of the European Technology Platform for Zero Emission Fossil Fuel Power Plants.

[49] W. Cole, A.W. Frazier, Cost projections for utility-scale battery storage, Technical Report NREL/TP-6A20-73222, National Renewable Energy Laboratory (NREL), Golden, CO, 2019, URL: https://www.nrel.gov/docs/fy19osti/73222.pdf.

[50] D. GL, Study on the import of liquid renewable energy: Technology cost assessment, 2020, URL: https://www.dnvgl.com. Prepared for Gas Infrastructure Europe (GIE).

[51] Energinet, European hydrogen backbone: How a dedicated hydrogen infrastructure can be created, 2020, URL: https://gasforclimate2050.eu/sdm_downloads/european-hydrogen-backbone/.

[52] Gas Infrastructure Europe, Guidehouse, Picturing the value of underground gas storage to the European hydrogen system, 2021, URL: https://www.gie.eu/publications/studies/. (Accessed 12 August 2025).

[53] Hordvei, Hummelen, EMPIRE-GreenHydrogen, 2024, https://github.com/3rl3nd/EMPIRE-SeasonalStorage.

[54] W.E. Hart, C.D. Laird, J.-P. Watson, D.L. Woodruff, G.A. Hackebeil, B.L. Nicholson, J.D. Siirola, et al., Pyomo-optimization modeling in python, vol. 67, Springer, 2017, http://dx.doi.org/10.1007/978-3-030-68928-5.

[55] Hordvei, Hummelen, EMPIRE-GreenHydrogen, 2024, https://github.com/3rl3nd/EMPIRE-GreenHydrogen.

[56] L. Gaudard, F. Romerio, F. Dalla Valle, R. Gorret, S. Maran, G. Ravazzani, M. Stoffel, M. Volonterio, Climate change impacts on hydropower in the swiss and Italian alps, Sci. Total Environ. 493 (2014) 1211–1221, http://dx.doi.org/10.1016/j.scitotenv.2013.10.012.

[57] R. Khalili, A. Khaledi, M. Marzband, A.F. Nematollahi, B. Vahidi, P. Siano, Robust multi-objective optimization for the Iranian electricity market considering green hydrogen and analyzing the performance of different demand response programs, Appl. Energy 334 (2023) 120737, http://dx.doi.org/10.1016/j.apenergy.2023.120737.

[58] M.M. Hayati, A. Aminlou, M. Abapour, M. Shafie-khah, H. Shahinzadeh, G.B. Gharehpetian, The power-to-X (PtX) effect in ancillary service markets: From opportunities and challenges toward future directions, Power- To- X Reg. Energy Syst. 432–451, http://dx.doi.org/10.1201/9781032719436-18.

[59] European Network of Transmission System Operators for Electricity (ENTSO-E), ENTSO-E statistical factsheet 2022, 2022, https://www.entsoe.eu/.

[60] Zero emissions platform, The cost of subsurface storage of CO2, 2020, URL: https://zeroemissionsplatform.eu/co2-storage-cost/.

[61] N. Zaccarelli, S. Giaccaria, M. Feofilovs, R.B. Lavin, The European natural gas demand database (ENaGaD), in: The European Natural Gas Demand database (ENaGaD) – An archive of daily time series from 2015 to 2020, 2021, http://dx.doi.org/10.2760/497677.

[62] European Network of Transmission System Operators for Electricity (ENTSO-E), TYNDP scenarios, 2023, https://www.entsos-tyndp-scenarios.eu/.